



H₂O and CO₂ in magmas from the Mariana arc and back arc systems

Sally Newman and Edward Stolper

Division of Geological and Planetary Sciences, California Institute of Technology, Pasadena, California 91125
(sally@gps.caltech.edu)

Robert Stern

Center for Lithospheric Studies, University of Texas at Dallas, Box 830688, MS FA31, Richardson, Texas 75083-0688

[1]. **Abstract:** We examined the H₂O and CO₂ contents of glasses from lavas and xenoliths from the Mariana arc system, an intraoceanic convergent margin in the western Pacific, which contains an active volcanic arc, an actively spreading back arc basin, and active behind-the-arc cross-chain volcanoes. Samples include (1) glass rims from Mariana arc, Mariana trough, and cross-chain submarine lavas; (2) glass inclusions in arc and trough phenocrysts; and (3) glass inclusions from a gabbro + anorthosite xenolith from Agrigan (Mariana arc). Glass rims of submarine arc lavas contain 0.3–1.9 wt % H₂O, and CO₂ is below detection limits. Where they could be compared, glass inclusions in arc phenocrysts contain more H₂O than their host glasses; most arc glasses and phenocryst inclusions contain no detectable CO₂, with the exception of those from a North Hiyoshi shoshonite, which contains 400–600 ppm. The glass inclusions from the Agrigan xenolith contain 4–6% H₂O, and CO₂ is below the detection limit. Glasses from the cross-chain lavas are similar to those from the arc: H₂O contents are 1.4–1.7 wt %, and CO₂ is below detection limits. Volatile contents in Mariana trough lava glass rims are variable: 0.2–2.8 wt % H₂O and 0–300 ppm CO₂. Glass inclusions from trough phenocrysts have water contents similar to the host glass, but they can contain up to 875 ppm CO₂. Volatile contents of melt inclusions from trough and arc lavas and from the xenolith imply minimum depths of crystallization of ~1–8 km. H₂O and CO₂ contents of Mariana trough glasses are negatively correlated, indicating saturation of the erupting magma with a CO₂–H₂O vapor at the pressure of eruption (~400 bars for these samples), with the vapor ranging from nearly pure CO₂ at the CO₂-rich end of the glass array to nearly pure H₂O at the H₂O-rich end. Degassing of these magmas on ascent and eruption leads to significant loss of CO₂ (thereby masking preeruptive CO₂ contents) but minimal disturbance of preeruptive H₂O contents. For submarine Mariana arc magmas, depths were low enough that degassing on ascent and eruption led to loss of both H₂O and CO₂; as a result, H₂O contents are positively correlated with water depth for these samples. The H₂O contents of primitive Mariana trough magmas richest in the slab-derived component (i.e., the most “arc-like” magmas) are ~2 wt %. Although evolved glasses with up to 4–6 wt % H₂O are present among Mariana arc samples, we interpret the glass inclusion data as indicating that primitive Mariana arc liquids contain 1–3 wt % H₂O. The preeruptive H₂O contents of primitive cross-chain seamount liquids are >1–2 wt %.

Keywords: Subduction; volatiles; basalts; Marianas; back arc basin; degassing.

Index terms: Major element chemistry; minor element chemistry; composition of the crust.

Received October 29, 1999; **Revised** March 27, 2000; **Accepted** March 31, 2000;

Published May 30, 2000.

Newman, S., E. Stolper, and R. Stern, 2000. H₂O and CO₂ in magmas from the Mariana arc and back arc systems, *Geochem. Geophys. Geosyst.*, vol. 1, Paper number 1999GC000027 [15,062 words, 9 figures, 6 tables]. May 30, 2000.

1. Introduction

[2]. Although much has been written about the importance of volatiles, particularly H₂O, in the generation, fractionation, and eruption of island arc, back arc, and continental arc magmas, until recently little was known of their concentrations in undegassed magmas from direct measurements. The principal difficulty has been that most sampled arc-related lavas erupt subaerially and consequently degas substantially, so preruptive volatile concentrations cannot usually be directly measured (although indirect constraints are available from experimentally determined phase relations [e.g., Sakuyama, 1983; Merzbacher and Egger, 1984; Sisson and Grove, 1993; Baker et al., 1994; Gardner et al., 1995; Danyushevsky et al., 1996]). Two things have changed in recent years: First, the development of microanalytical tools has enabled measurement of the concentrations of volatiles in glass inclusions within phenocrysts, which frequently remain sealed during eruption and therefore preserve preruptive volatile contents [Metrich et al., 1993; Sisson and Layne, 1993; Sobolev and Danyushevsky, 1994; Sobolev and Chaussidon, 1996; Hauri, 1998; Sisson and Bronto, 1998]; and second, submarine arc-related lavas have become increasingly available, and they can preserve preruptive volatile contents because they degas incompletely on eruption under water at pressures of up to several hundred bars [Stern and Bibe, 1984; Devine and Sigurdsson, 1995; Dixon et al., 1995].

[3]. In this paper, we take advantage of both of these developments to provide additional constraints on the concentrations and roles of H₂O

and CO₂ in the generation of magmas from the Mariana arc and its associated back arc system. We use the microanalytical capability of Fourier transform infrared spectroscopy (FTIR) to measure the concentrations of these volatiles in the glassy rims of submarine flows and in melt inclusions trapped in crystalline phases. Important features of our work are the measurement of CO₂ in these samples and the fact that they come from a variety of environments (i.e., the magmatic front of the arc; cross-arc seamount chains extending to the rear of the magmatic front; and the back arc basin). These features allow characterization of the preruptive concentrations of both of the major volatiles (i.e., H₂O and CO₂) in magmas from this oceanic arc/back arc region and examination of differences between subenvironments within this overall system.

2. Sample Description

2.1. Mariana Trough (Back Arc)

[4]. Samples were available from a substantial length of the Mariana trough axis, from the intersection of the back arc spreading center with the arc at ~23°N, south to ~15°N (Figure 1). The nature of crustal extension and magmatism varies over the length of the extension axis, from rifting associated with the eruption of arc-like evolved lavas and porphyritic basalts in the shallow (i.e., near sea level) north to seafloor spreading and eruption of mid-ocean ridge basalt (MORB)-like lavas in the central and southern portions of the trough, where depths to the ridge axis range from 3.5 km at 13°N to 4.5–5 km at 20°–21°N [Martinez et al., 1995; Gribble et al., 1996, 1998]. Lavas from the full range of tectonic settings and

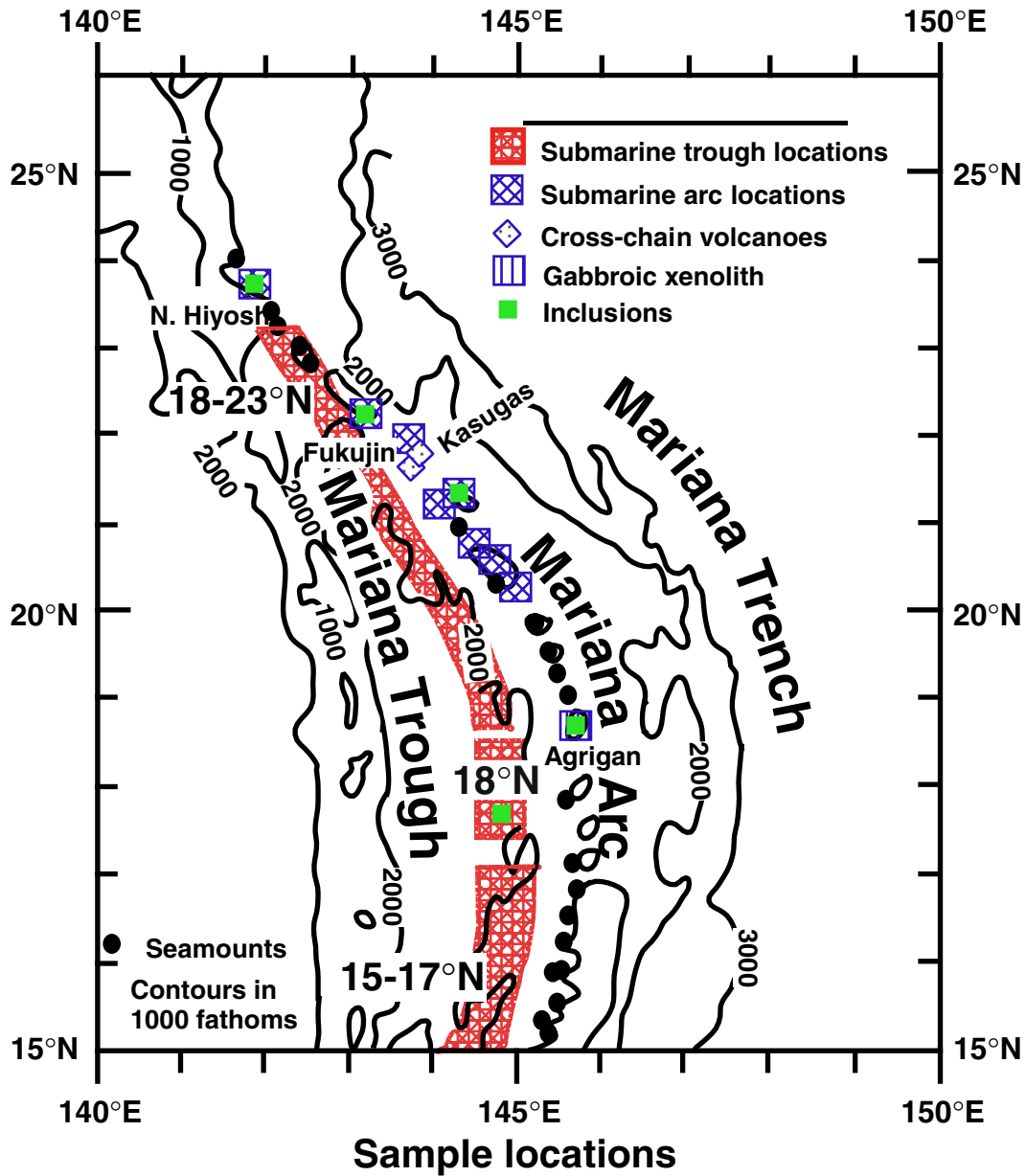


Figure 1. Location map for samples included in this study. For the trough, individual sample locations are too numerous to show separately. Therefore just the ranges are shown.

spanning the range of known magma types from the trough are included in this study.

[5] Samples were collected by dredge (WOK series) and the *Alvin* submersible (ALV series)

from near 18°N by James Hawkins (Scripps Institution of Oceanography) during a 1987 cruise of the R/V *Atlantis II* (major and trace elements reported by *Hawkins et al.* [1990]; volatile data initially published by *Stolper and*



Newman [1994]); by dredge from the same region during the 1988 GH88-1 cruise of the Hakurei-Marui (samples D1009 and D1010; major elements and rare gases are reported by Ikeda *et al.* [1998]); by dredge (DS and GTVA series) from near 15° to 17°N by S. Bloomer (Oregon State University) and D. Steuben (Karlsruhe University) during a 1990 cruise of the R/V *Sonne of Germany* (H₂O contents and major and trace element and isotopic compositions are given by Gribble *et al.* [1996]); and by dredge from 18° to 23°N during Leg 7 of the 1991 TUNES expedition of the R/V *Thomas Washington* (dredges 46–82; H₂O contents and major and trace element and isotopic compositions are given by Gribble *et al.* [1998]). Sampling locations, full sample names, and depths of collection for the trough samples are listed in Table 1. Petrographic descriptions of samples from most of these suites are given by Hawkins *et al.* [1990] and Gribble *et al.* [1996, 1998]; the suite from which samples D1009 and D1010 come is described (although in somewhat less detail) by Ikeda *et al.* [1998].

[6] Fresh basaltic glass was picked from the glassy lavas, all of which were fragments of pillow rinds, except for GTVA 71-1-7, which is from a sheet flow. Most analyzed chips contain at least one vesicle, generally >100 μm across. The glass fragments contain crystals in varying proportions, primarily olivine and plagioclase phenocrysts and plagioclase microlites; some fragments show evidence of devitrification/crystallization locally around these crystals, and such regions were avoided during analysis. Many of the olivine and plagioclase phenocrysts are >1 mm across and contain inclusions of brown glass. Most of these glass inclusions, especially in plagioclase, are at least partially devitrified and appear to be connected to a crystal face by a capillary [Anderson, 1991]. We analyzed four glassy inclusions in three olivine phenocrysts from WOK 28-3; none of these have visible connections to grain bound-

aries. Two plagioclase-hosted glassy inclusions were also analyzed: one, in plagioclase from ALV 1833-1, is connected to the crystal–host glass interface by a capillary; the other, in plagioclase from ALV 1832-2, appears to have been isolated from the host liquid since entrapment. Representative photomicrographs of these inclusions are shown in Figure 2.

2.2. Mariana Arc (Magmatic Front)

[7] Samples were available from a substantial length of the Mariana arc: from North Hiyoshi (23.37°N), near the northern end of the arc just north of where it is intersected by the Mariana trough, to Agrigan (~18.75°N), in the central region of the arc (Figure 1). With the exception of a composite gabbro + anorthosite xenolith from Agrigan island, the samples are all submarine lavas dredged from seamounts by one of us (R. Stern) and S. Bloomer during the 1985 TT-192 cruise of the R/V *T. G. Thompson*. Geochemical data for these samples are given by Bloomer *et al.* [1989a, 1989b], Lin *et al.* [1989], and S. H. Bloomer and R. J. Stern (unpublished data, 1999). No H₂O or CO₂ measurements have been reported for these samples, but Garcia *et al.* [1979] reported measurements from samples dredged from Fukujin seamount (21.92°N). The samples studied here include low-K and medium-K series lavas with compositions ranging from basalt to dacite or silicic andesite [Bloomer *et al.*, 1989a]. Lavas from the northernmost seamounts (from dredges 53 and 54) are shoshonitic; these lavas may relate to the propagation of the trough spreading center into the arc [Bloomer *et al.*, 1989a]. Sampling locations, full sample names, and depths of collection (for the lavas) for the arc samples are listed in Table 3.

[8] The dredged lavas are generally porphyritic and vesicular. The groundmass in most samples is partly crystalline, but glass fragments

Table 1. Dissolved Volatile Contents and Depths of Collection and Calculated Vapor Saturation Conditions^a for Mariana Trough Matrix Glasses

Sample	Latitude, °N	Longitude, °E	H ₂ O, wt %	CO ₂ , ppm	Depth of Collection, m	Vapor-Saturated Depth ^b , m	X(H ₂ O) _{vapor} ^c
<i>15°–17°N^d</i>							
DS18-1-6	16.18	144.79	2.03 ± 0.06	30 ± 9	3838–4052	4600	0.87
DS22-2-2	16.96	144.78	0.48 ± 0.01	168 ± 6	3055–3287	3600	0.06
DS74-2-1	16.53	144.83	2.08 ± 0.10	28 ± 33	3880–5000	4700	0.88
DS74-2-3	16.53	144.83	2.16 ± 0.12	bdl ^e	3880–5000	4500	1.00
DS74-3-1	16.53	144.83	1.40 ± 0.08	95 ± 4	3880–5000	3800	0.50
DS79-2-2	16.08	144.74	1.09 ± 0.06	152 ± 2	3625–3747	4200	0.27
DS80-23-2	15.75	144.75	1.52 ± 0.15	98 ± 2	3730–3922	4200	0.53
DS80-25-3	15.75	144.75	2.78 ± 0.08	104 ± 10	3730–3922	9500	0.78
DS84-1-1	15.00	144.46	0.20 ± 0.003	188 ± 11	4046–4272	3900	0.01
DS84-2-1	15.00	144.46	0.21 ± 0.004	215 ± 6	4046–4272	4400	0.01
DS86-4-1	15.09	144.50	0.58 ± 0.01	126 ± 21	3386–3518	2900	0.10
DS88-1-2	15.30	144.51	1.30 ± 0.07	199 ± 6	4279–4671	5700	0.29
DS88-2-1	15.30	144.51	1.04 ± 0.05	161 ± 31	4279–4671	4300	0.24
DS88-3-1	15.30	144.51	1.24 ± 0.02	189 ± 12	4279–4671	5300	0.28
GTVA 71-1-7	16.99	144.83	1.34 ± 0.14	111 ± 19	3400–3404	4000	0.44
GTVA 73-2-2	16.69	144.82	1.46 ± 0.09	142 ± 4	4124–4236	5000	0.42
GTVA 75-1-1	16.41	144.85	2.21 ± 0.07	bdl	3670–3954	4900	1.00
<i>18°N^f</i>							
WOK 5-4	18.3	144.7	1.60 ± 0.05	64 ± 6	3925	3800	0.66
WOK 10-1	18.4	144.65	1.14 ± 0.02	120 ± 1	3950–4100	3700	0.34
WOK 16-2	18.1	144.75	0.64 ± 0.01	184 ± 7	3969–3975	4100	0.09
WOK 28-3	17.6	144.9	0.50 ± 0.01	183 ± 10	4050–4126	4000	0.05
ALV 1832-2	18.15	144.8	2.28 ± 0.09	18 ± 5	3694	5300	0.93
ALV 1833-1	18.1	144.75	2.43 ± 0.05	24 ± 15	3691	6100	0.92
ALV 1833-11	18.1	144.75	1.20 ± 0.01	102 ± 12	3693	3400	0.40
ALV 1839-21	18.2	144.7	1.21 ± 0.03	94 ± 6	4044	3300	0.42
ALV 1840-3	18.2	144.7	1.26 ± 0.04	113 ± 33	3283	3800	0.40
ALV 1846-9	18.3	144.7	1.89 ± 0.05	bdl	3485	3400	1.00
ALV 1846-12	18.3	144.7	1.55 ± 0.02	90 ± 8	3751	4200	0.56
<i>18°–23°N^g</i>							
46:1-6	20.82	143.55	1.41 ± 0.09	111 ± 9	3700	4200	0.46
47:1-5	20.97	143.44	1.76 ± 0.08	66 ± 6	3680–5100	4300	0.69
48:1-3	21.31	143.36	1.56 ± 0.10	bdl	2860–2900	2400	1.00
54:1-1	22.79	142.42	1.69 ± 0.02	61 ± 6	3430–3460	4000	0.69
55:1-1	22.87	142.32	1.79 ± 0.06	bdl	3125–3205	3600	1.00
68:1-2	21.35	143.28	1.84 ± 0.08	69 ± 6	3800–3900	4700	0.70
71:1-14	20.31	143.93	1.82 ± 0.36	128 ± 17	4330–4400	5800	0.56
72:2	19.83	144.3	2.23 ± 0.09	74 ± 13	4380–4450	6300	0.77
73:2-1	19.73	144.4	1.15 ± 0.05	160 ± 19	3600–4036	4500	0.28
74:1-1	19.67	144.39	1.00 ± 0.06	112 ± 4	3630–3690	3200	0.29
75:1-2	19.44	144.48	0.72 ± 0.02	227 ± 1	4380–4450	5100	0.09
76:1-1	19.45	145.54	0.73 ± 0.01	180 ± 16	3364–4480	4100	0.12
80:1-3	19.12	144.67	0.57 ± 0.003	295 ± 7	4040–4050	6300	0.05
82:1-1	18.75	144.66	1.69 ± 0.20	109 ± 18	4300–4340	5000	0.56
D1009	18.15	144.73	1.20 ± 0.03	138 ± 2	3700–3770	4200	0.33
D1010	18.15	144.73	1.13 ± 0.07	139 ± 1	3700–3770	4000	0.30
Std JDF-D2			0.347 ± 0.007	225 ± 45			



large enough for analysis were picked from all samples except 38-2, in which the plagioclase-rich groundmass was microcrystalline. These samples contain phenocrysts of olivine, clinopyroxene, plagioclase, orthopyroxene, hornblende, and/or biotite (in the shoshonites), many of which contain melt inclusions. Ten glassy inclusions with no evidence of connection to a grain boundary were analyzed from four different submarine arc samples. Each of these inclusions was in a separate olivine, plagioclase, or clinopyroxene host crystal. Photomicrographs of two of these inclusions are shown in Figure 2, one showing a large vapor bubble.

[9] The Agrigan xenolith was collected by R. Stern in 1976 and described by *Stern* [1979]. It is a cumulate comprising distinct anortho-

sitic and gabbroic layers. We studied five glass inclusions from five different cumulus olivine grains from this sample. These inclusions have no visible connections to the surfaces of their host olivines. A representative photomicrograph of one of these inclusions is shown in Figure 2, showing daughter crystals growing in from the inclusion boundary.

2.3. Cross-Chain Seamount Samples

[10] Glassy samples from the Kasuga cross-chain at ~21.5°N [*Fryer et al.*, 1997] were studied. Sampling locations and depths of collection for these samples are listed in Table 3. No glass inclusions within phenocrysts were analyzed from these samples. There are no previous measurements of volatile contents in these or related samples.

Notes to Table 1:

^a Pressures for vapor saturation and the composition of the coexisting vapor in the mixed volatile system were calculated using the following relationship describing the thermodynamic condition for saturation:

$$\frac{a_{\text{H}_2\text{O}}^m / f_{\text{H}_2\text{O}}^v}{K_{\text{H}_2\text{O}}} + \frac{a_{\text{CO}_2}^m / f_{\text{CO}_2}^v}{K_{\text{CO}_2}} = 1,$$

where a is activity, m is melt, mol is molecular, v is vapor, f is fugacity of the pure volatile component at the pressure and temperature of interest, K is solubility constant for the pure volatile component adjusted to the appropriate temperature and pressure. The solubility of H₂O is described in terms of the molecular H₂O species, according to *Stolper* [1982]. Assuming Henrian behavior, the activities can be taken to be equal to the mole fractions. Mixing between the components of the vapor phase is assumed to be ideal, following *Dixon and Stolper* [1995]. The relationship given above was used to calculate saturation curves for mixed H₂O–CO₂ volatile phases for several pressures. Fugacities of pure H₂O and CO₂ were calculated using a modified Redlich-Kwong model [*Holloway*, 1977] and their solubilities are from *Dixon et al.* [1995]. The calculations were done at 1150°C, which is a reasonable temperature for Mariana trough basalts, based on the results of *Hawkins et al.* [1990] and *Hawkins and Melchior* [1985], who calculated magmatic temperatures of 1078°–1199°C based on olivine/chromite and olivine/glass geothermometers. This relationship was also used to calculate the saturation curves for mixed H₂O–CO₂ volatile phases for several pressures shown in Figure 5.

^b Calculated depth of vapor saturation for reported H₂O and CO₂ contents based on calculated pressure of vapor saturation (see footnote a) and converting to water depth using 10-m water depth = 1 bar. Calculated depths have been rounded to the nearest 100 m.

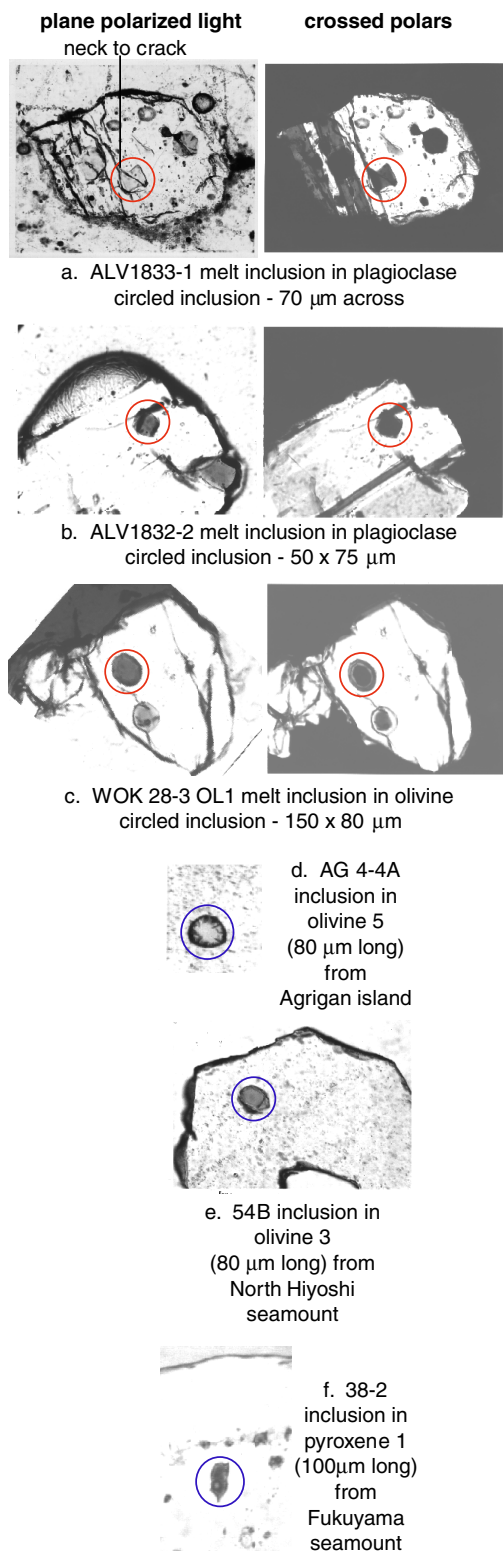
^c Calculated mole fraction of H₂O in vapor coexisting with melt with reported H₂O and CO₂ contents (assumed to be 1 if CO₂ is below detection limit). See footnote a.

^d All these samples formally require the prefix “Sonne 69”; i.e., DS18-1-6 is Sonne 69 DS18-1-6. The prefixes have been omitted for simplicity. DS refers to dredge sample, and GTVA refers to grab television apparatus.

^e In all tables, bdl is below detection limit.

^f These same samples were previously analyzed by *Stolper and Newman* [1994]. The WOK samples are dredges; the ALV samples were collected with the *Alvin* submersible. Results reported here are averages of these previous results and measurements on new sections of these samples prepared for this study. CO₂ contents were determined as described in the text using a less subjective approach to background subtraction. CO₂ contents presented here differ on average by +6% (relative) compared to the results presented by *Stolper and Newman* [1994], although individual analyses can deviate by up to plus or minus several tens of percent (relative). Excluding H₂O-rich samples ALV 1832-2 and ALV 1833-1, reported water contents are on average 0.3% (relative) higher than the results presented by *Stolper and Newman* [1994].

^g The D1009 and D1010 samples formally require the prefix “GH88-1”; i.e., D1009 is GH88-1 D1009. The D indicates they are dredge samples. All other samples in this section formally require the prefix “TUNES7 D,” where again the D indicates they are from dredges. The prefixes have been omitted for simplicity.



[11] The three Kasuga seamounts form a ridge that trends obliquely away from the northern part of the arc to the SSW (Figure 1). The closest active volcano in the arc itself is Fukujin, located ~ 30 km NW of the Kasugas. The three Kasuga seamount samples included in this study were collected from the lower to middle slopes of Kasuga 2 and Kasuga 3 by the submersible *Alvin* in 1987 as described by Fryer *et al.* [1997]. These two seamounts are active, on the basis of the occurrence of hydrothermal activity and fresh glass on both [Fryer *et al.*, 1997]. The two Kasuga 2 samples in this study are high-K basalts, and the one Kasuga 3 sample is an absarokite. Petrographic descriptions and geochemical data for the suite of Kasuga samples, including those studied here, are given by Jackson [1989], Stern *et al.* [1993], and Fryer *et al.* [1997]. Lavas from these seamounts have glassy margins from which clean glass was picked; the samples we studied are vesicular (~ 5 –50%) and aphyric to sparsely phyric (with phenocrysts of olivine, plagioclase, and clinopyroxene) [Stern *et al.*, 1993; Fryer *et al.*, 1997].

3. Analytical Techniques

3.1. H₂O and CO₂

[12] For each fragment of glassy lava a doubly polished section ~ 0.5 –2 mm across and ~ 50 –320 μm thick was prepared. For glass inclusions in phenocrysts the host phase was doubly polished, exposing the inclusion on both sides; after polishing, the inclusions were ~ 15 –120 μm across and ~ 10 –100 μm thick. Dissolved H₂O and CO₂ contents were determined using the FTIR techniques described by

Figure 2. Photomicrographs of representative melt inclusions in phenocrysts from submarine Mariana trough and arc lavas and in olivine from the Agrigan xenolith.

Table 2. Volatile Concentrations in Mariana Trough Glass Inclusions

Sample	H ₂ O, wt %	CO ₂ , ^a ppm	Pressure for Vapor Saturation, ^b bars	X(H ₂ O) _{vapor} ^c
WOK 28-3 (in OL1)	0.47 ± 0.02	691 ± 28	1400	0.02
WOK 28-3 (in OL2)	0.48 ± 0.04	613 ± 78	1200	0.02
WOK 28-3 (large inclusion in OL3)	0.60 ± 0.09	-		
WOK 28-3 (small inclusion in OL3)	0.55 ± 0.01	-		
ALV 1832-2 (in PLAG)	2.23 ± 0.07	875 ± 141	2200	0.25
ALV 1833-1 (in PLAG)	1.71 ± 0.01	bdl	300	1.00

^a Dash indicates a sample in which the CO₂ content was not determined due to large interference fringes in the infrared spectrum. The pressure of vapor saturation and composition of coexisting vapor were not calculated for these samples. Here bdl indicates the CO₂ content was below the detection limit.

^b Calculated pressure of vapor saturation for reported H₂O and CO₂ contents (0% CO₂ assumed for samples in which CO₂ is bdl). See footnote a, Table 1. Calculated pressures have been rounded to the nearest 100 bars.

^c Calculated mole fraction of H₂O in vapor coexisting with melt with reported H₂O and CO₂ contents (assumed to be 1 if CO₂ is bdl). See footnote a, Table 1.

Fine and Stolper [1985/1986] and *Dixon et al.* [1988], except most spectra were taken with a Nicolet IR-Plan microscope attached to a Nicolet 60SX spectrometer. The double-aperture system on the microscope [*Wopenka et al.*, 1990] was used, with adjustable rectangular apertures ranging from ~15–110 μm across: apertures were positioned above and below the sample to mask light not propagating through the region of interest and to eliminate light refracted significantly from normal while passing through the sample. In this configuration the region of interest can be seen through the Cassegrainian optics of the microscope, which are also used to direct the infrared beam.

[13] The absorption bands used to determine dissolved H₂O concentrations were the OH stretching band at ~3550 cm⁻¹ (primarily for determining molecular H₂O plus hydroxyl contents of glasses with total H₂O contents less than ~1 wt %, although it was also used for a few thin samples with higher total H₂O contents), the ~5200 cm⁻¹ band resulting from the combination stretching and bending mode of H₂O molecules, and the ~4500 cm⁻¹ band resulting from the combination modes of X–OH groups (where X = Si, Al, etc. [*Stolper*, 1982]). The antisymmetric stretching bands of distorted CO₃²⁻ groups at 1515 and 1435 cm⁻¹

were used to determine the amount of CO₂ dissolved as carbonate ions. Except for the most silicic samples (see footnotes to Tables 3 and 4), a molar absorptivity of 63 ± 3 L/mol cm (P. Dobson, S. Newman, S. Epstein, and E. Stolper, unpublished data, 1987) was used to calculate H₂O concentrations from the intensity of the 3550 cm⁻¹ band; this is similar to the value of *Pandya et al.* [1992] (61 ± 1 L/mol cm) and *Yamashita et al.* [1997] (64 ± 1 L/mol cm), but lower than that reported by *Jendrzewski et al.* [1996b] (78 ± 1 L/mol cm). Molar absorptivities of 0.67 ± 0.03 and 0.62 ± 0.07 L/mol cm were used (except for the most silicic samples; see footnotes to Tables 4 and 5) to calculate the molecular H₂O and hydroxyl group concentrations from the 5200 and 4520 cm⁻¹ bands [*Dixon et al.*, 1995]. A molar absorptivity of 375 ± 20 L/mol cm [*Fine and Stolper*, 1985/1986] was used to calculate the concentration of CO₂ dissolved as CO₃²⁻; this value is similar to the 397 ± 7 L/mol cm value of *Jendrzewski et al.* [1996a]. The density of each glass was assumed to be 2.8 g/cm³. The absence of absorption features at 2350 cm⁻¹ indicates that dissolved molecular CO₂ is below the detection limit in all samples (typically less than ~25 ppm for samples in the thickness range used here), consistent with previous observations that CO₂ dissolves nearly entirely as



Table 3. Volatile Concentrations in Submarine Mariana-Arc-Lava Matrix Glasses and Cross-Chain–Volcano Matrix Glasses

Sample	Volcano	Latitude, °N	Longitude, °E	H ₂ O, wt %	CO ₂ , ppm	Depth of Col- lection, m	Vapor-Satu- rated Depth at 0% CO ₂ , ^a m	Vapor-Saturated Depth at 50 ppm CO ₂ , ^b m	Model CO ₂ , ^c ppm
<i>Mariana Arc Seamounts^d</i>									
14-21 (basaltic andesite)	supply reef	20.13	144.08	0.75 ± 0.09	bdl	530–1060	500	1500	15
14-24 (basaltic andesite)	supply reef	20.13	144.08	0.28 ± 0.08	bdl	530–1060	60	1100	36
21-8 (basaltic andesite)	NW Uracas	20.65	144.44	1.18 ± 0.10	bdl	2000–2200	1300	2300	39
25-14 (andesite)	S. Daikoku	21.05	144.50	0.80 ± 0.07	bdl	1430–1450	600	1600	42
29:1-2 (silicic andesite) ^e	Daikoku	21.33	144.19	0.75 ± 0.06	bdl	400–920	700	1800	-
29:2-2 (silicic andesite) ^e	Daikoku	21.33	144.19	0.40 ± 0.02	bdl	400–920	200	1300	21
34-2-2 (basaltic andesite)	Fukujin	21.92	143.46	0.44 ± 0.08	bdl	1002–1600	160	1200	55
34-3-3 (basaltic andesite)	Fukujin	21.92	143.46	0.62 ± 0.01	bdl	1002–1600	330	1400	47
38-2 (basalt) ^f	Fukuyama	22.37	143.12			1740–1800			
39-1 (magnesian andesite)	Sakoyama	22.36	143.08	1.06 ± 0.06	bdl	2100	1000	2100	52
53i (rhyolite) ^e	N. Hiyoshi	23.37	141.80	1.91 ± 0.18	bdl	1280–1687	4000	5200	-
54B (basalt)	N. Hiyoshi	23.37	141.72	0.91 ± 0.08	bdl	1250–1640	700	1800	34
54G (basalt)	N. Hiyoshi	23.37	141.72	0.94 ± 0.06	bdl	1250–1640	800	1800	31
<i>Kasuga Cross-Chain Seamounts</i>									
ALV 1880-3 (high-K basalt)	Kasuga 2	21.58	~143.6	1.45 ± 0.01	bdl	2200–2600	2000	3000	20
ALV 1880-5 (high-K basalt)	Kasuga 2	21.58	~143.6	1.55 ± 0.22	bdl	2200–2600	2300	3300	6
ALV 1884-10 (absarokite)	Kasuga 3	21.37	~143.5	1.69 ± 0.13	bdl	2900–3500	2700	3800	23

^a Calculated depth of vapor saturation for reported H₂O content and 0% CO₂ based on calculated pressure of vapor saturation (see footnote a, Table 1) and converting to water depth using 10-m water depth = 1 bar.

^b Calculated depth of vapor saturation for reported H₂O content and 50 ppm CO₂ based on calculated pressure of vapor saturation (see footnote a, Table 1) and converting to water depth using 10 m water depth = 1 bar. Calculated depths have been rounded to the nearest 100 m.

^c Calculated CO₂ content required for vapor saturation at the depth of collection (see footnote a, Table 1). For dredged samples, this calculation was done for the midpoint of the depth range of the dredge. No value is listed for 53i because it is oversaturated with respect to pure H₂O vapor at the depth of collection (see Figure 4a).

^d All Mariana arc seamount samples formally require the prefix “TT192 D”; i.e., 14-21 is TT192 D14-21. The prefixes have been omitted for simplicity.

^e For these silicic samples, values of molar absorptivities appropriate to rhyolitic glass [Newman *et al.*, 1986; Dobson *et al.*, 1989] were used to determine dissolved H₂O contents. Calculations of vapor saturation utilized the solubility model for rhyolitic melts from Blank *et al.* [1993].

^f No glass available for this sample. Consequently, no measured volatile contents or calculated pressures or CO₂ contents at vapor saturation are given.

Table 4. Volatile Concentrations in Mariana Arc Glass Inclusions

Sample	H ₂ O, wt %	CO ₂ , ^a ppm	Pressure for Vapor Saturation (0% CO ₂ If bdl), ^b bars	Pressure for Vapor Saturation (50 ppm CO ₂ If bdl), ^c bar	X(H ₂ O) _{vapor} ^d
<i>Inclusions in Lavas</i>					
29:2-2 (in PLAG1) ^e	1.89 ± 0.06	-			
29:2-2 (in PLAG2) ^e	2.02 ± 0.07	bdl	400	500	1.00
38-2 (in CPX1)	3.30 ± 0.16	-			
38-2 (in CPX2)	2.55 ± 0.18	-			
54B (in OL1)	1.43 ± 0.20	581 ± 60	1400	1400	0.16
54B (in OL2)	1.89 ± 0.06	612 ± 103	1600	1600	0.25
54B (in OL3)	2.28 ± 0.04	393 ± 51	1300	1300	0.41
54B (in OL4)	2.49 ± 0.10	-			
54G (in PLAG1)	2.20 ± 0.04	-			
54G (in PLAG2)	1.96 ± 0.07	-			
<i>Inclusions in Xenolith</i>					
AG4-4A (in OL1)	5.11 ± 0.20	bdl	2200	2300	1.00
AG4-4A (in OL2)	5.57 ± 0.25	-			
AG4-4A (in OL3)	4.05 ± 0.14	-			
AG4-4A (in OL4)	5.48 ± 0.64	-			
AG4-4A (in OL5)	5.19 ± 0.12	-			

^a Dash indicates a sample in which the CO₂ content was not determined due to large interference fringes in the infrared spectrum. The pressure of vapor saturation and composition of coexisting vapor were not calculated for these samples. Here “bdl” indicates the CO₂ content was below the detection limit.

^b Calculated pressure of vapor saturation for reported H₂O and CO₂ contents (0% CO₂ assumed for samples in which CO₂ is bdl). See footnote a, Table 1. Calculated pressures have been rounded to the nearest 100 bars.

^c Calculated pressure of vapor saturation for reported H₂O and CO₂ contents (50 ppm CO₂ assumed for samples in which CO₂ is bdl). See footnote a, Table 1. Calculated pressures have been rounded to the nearest 100 bars.

^d Calculated mole fraction of H₂O in vapor coexisting with melt with reported H₂O and CO₂ contents (assumed to be 1 if CO₂ is bdl). See footnote a, Table 1.

^e For these silicic samples, values of molar absorptivities appropriate to rhyolitic glass [Newman *et al.*, 1986; Dobson *et al.*, 1989] were used to determine dissolved H₂O contents. Calculations of vapor saturation utilized the solubility model for rhyolitic melts from Blank *et al.* [1993].

carbonate ions in basaltic glasses [Fine and Stolper, 1985/1986].

[14] Procedures for processing spectra to determine carbonate concentrations were modified from those described by Dixon *et al.* [1988] in order to minimize subjectivity in subtracting baselines and overlapping bands in the region of the spectrum in which the carbonate bands occur. For each spectrum we determined a least squares fit of the spectrum in the region of the carbonate bands (1800–1350 cm⁻¹) to the sum of four components: the spectrum of a devolatilized basaltic glass (quenched from a sample of molten WOK-16-2 held on a Pt loop at 1300°C, 1 atm, and an *f*O₂ at the QFM buffer for 15 min); a band at 1630 cm⁻¹ (the funda-

mental bending mode of H₂O molecules); a carbonate doublet at 1515 and 1435 cm⁻¹; and a linear background component with variable slope and intercept. The 1630 cm⁻¹ band was modeled using the shape of the band in a spectrum of a H₂O-rich, carbonate-poor sample (DS74-2-3) after subtraction of the silicate baseline and normalization of the maximum absorbance of the resultant band to 1. A similar procedure was used to generate a model spectrum for the carbonate doublet from the spectrum of a carbonate-rich sample (DS84-1-1); this sample contains little H₂O (0.20 wt %) and therefore does not display a significant molecular H₂O band at 1630 cm⁻¹, but a small correction for the contribution of such a band was made using the band shape from DS74-2-3.



Table 5. Compositions of Glass Inclusions (by Electron Microprobe)

	ALV 1832-2 (in PLAG)	ALV 1833-1 (in PLAG)	WOK 28-3 (in OL1)	WOK 28-3 (in OL2)	WOK 28-3 (Large Inclu- sion in OL3)	WOK 28-3 (Small Inclu- sion in OL3)	Average VG-2 <i>n</i> = 8 ^a
<i>Mariana Trough Glass Inclusions</i>							
SiO ₂	51.42	50.33	49.77	49.13	47.63	47.79	50.12 ± 0.37
Al ₂ O ₃	13.42	15.14	16.23	15.38	15.73	15.54	13.76 ± 0.14
TiO ₂	1.36	1.05	1.28	1.26	1.52	1.48	1.81 ± 0.14
MgO	7.85	7.13	7.02	6.01	6.02	4.89	6.99 ± 0.06
CaO	9.55	9.12	12.02	12.13	10.94	11.39	10.83 ± 0.06
FeO	9.04	7.42	8.33	10.46	11.20	11.53	11.59 ± 0.24
MnO	0.19	0.15	0.16	0.20	0.15	0.25	0.20 ± 0.03
Na ₂ O	2.62	3.62	3.32	3.23	4.16	3.84	2.82 ± 0.06
K ₂ O	0.27	0.42	0.11	0.10	0.10	0.06	0.21 ± 0.02
H ₂ O	2.23	1.71	0.47	0.48	0.60	0.55	
Cl	nd ^b	nd	nd	nd	nd	nd	
Total	97.95	96.09	98.71	98.38	98.05	97.32	98.37 ± 0.37
	29:2-2 (in PLAG1)	29:2-2 (in PLAG2)	38-2 (in CPX1)	54B (in OL3)	54G (in PLAG1)	54G (in PLAG2)	
<i>Mariana Arc Lava Glass Inclusions</i>							
SiO ₂	65.67	64.68	51.50	47.75	62.99	62.85	
Al ₂ O ₃	13.86	13.21	13.51	15.39	16.40	16.79	
TiO ₂	0.68	0.70	0.71	1.07	0.44	0.45	
MgO	0.69	0.87	7.25	4.84	0.78	0.81	
CaO	2.68	3.02	12.12	9.29	1.61	1.74	
FeO	4.97	4.58	9.77	11.41	3.16	3.27	
MnO	0.16	0.11	0.25	0.26	0.12	0.15	
Na ₂ O	3.54	4.35	1.37	3.24	4.05	3.59	
K ₂ O	2.70	2.77	0.34	2.01	5.98	5.38	
H ₂ O	1.89	2.02	3.30	2.28	2.20	1.96	
Cl	nd	nd	nd	0.16	0.38	0.41	
Total	96.84	96.31	100.1	97.54	97.73	96.99	
	AG4-4A (in OL1)	AG4-4A (in OL2)	AG4-4A (in OL3)	AG4-4A (in OL4)	AG4-4A (in OL5)		
<i>Mariana Arc Xenolith Glass Inclusions</i>							
SiO ₂	50.13	50.32	49.31	49.17	49.24		
Al ₂ O ₃	17.84	17.85	17.15	17.14	18.01		
TiO ₂	0.97	0.94	0.84	0.93	0.64		
MgO	2.16	1.98	4.06	2.59	2.63		
CaO	11.61	11.50	11.10	11.09	11.99		
FeO	7.53	7.28	8.57	7.65	7.66		
MnO	0.20	0.19	0.17	0.20	0.16		
Na ₂ O	2.34	1.99	2.33	2.14	2.00		
K ₂ O	0.41	0.44	0.37	0.39	0.36		
H ₂ O	5.11	5.57	4.05	5.48	5.19		
Cl	nd	nd	nd	nd	nd		
Total	98.3	98.06	97.95	96.78	97.88		

^a Analysis of VG-2 standard glass, with 1σ uncertainties based on multiple analyses (*n* = 8).

^b The nd indicates that Cl was not determined for this sample.

The coefficient for the model carbonate doublet from the least squares fit to each spectrum was

used to calculate the dissolved CO₃²⁻ content (as CO₂); a representative spectrum and its least

Table 6. Compositions of Host Minerals of Glass Inclusions (by Electron Microprobe)

	PLAG (ALV 1832-2)	PLAG (ALV 1833-1)	OL1 (WOK 28-3)	OL2 (WOK 28-3)	OL3 (WOK 28-3)		
<i>Host Minerals of Mariana Trough Glass Inclusions</i>							
SiO ₂	48.32	46.00	39.88	38.58	38.30		
Al ₂ O ₃	32.18	33.77	0.04	0.06	0.07		
TiO ₂	0.03	0.04	0.00	0.02	0.02		
MgO	0.18	0.11	47.02	45.52	41.35		
CaO	16.14	17.53	0.29	0.32	0.35		
FeO	0.40	0.43	13.14	15.59	17.38		
MnO	0.00	0.01	0.20	0.26	0.28		
Na ₂ O	2.32	1.36	0.00	0.01	0.17		
K ₂ O	0.03	0.02	0.02	0.01	0.02		
Total	99.60	99.27	100.59	100.37	97.94		
An, Fo	An77.0	An85.3	Fo85.3	Fo83.2	Fo79.8		
	PLAG2 (29:2-2)	CPX1 (38-2)	OL1 (54B)	OL3 (54B)	OL4 (54B)	PLAG1 (54G)	PLAG2 (54G)
<i>Host Minerals of Mariana Arc Lava Glass Inclusions</i>							
SiO ₂	52.69	51.83	38.16	37.05	38.01	54.58	55.23
Al ₂ O ₃	28.39	2.27	0.09	0.05	0.04	28.05	27.48
TiO ₂	0.03	0.27	0.02	0.02	0.02	0.07	0.02
MgO	0.08	17.10	38.99	39.61	39.41	0.05	0.07
CaO	11.39	20.90	0.30	0.29	0.31	10.39	9.63
FeO	0.63	6.03	23.68	22.90	23.15	0.57	0.38
MnO	0.00	0.15	0.43	0.46	0.46	0.00	0.04
Na ₂ O	4.80	0.12	0.00	0.01	0.01	5.33	5.52
K ₂ O	0.24	0.01	0.02	0.01	0.02	0.72	0.79
Total	98.25	98.68	101.69	100.40	101.43	99.76	99.16
An, Fo or En/Fs	An54.3	En45.4 Fs14.3	Fo73.8	Fo74.7	Fo74.4	An48.4	An45.9
	OL2 (AG4-4A)	OL3 (AG4-4A)	OL4 (AG4-4A)	OL5 (AG4-4A)			
<i>Host Minerals of Mariana Arc Xenolith Glass Inclusions</i>							
SiO ₂	38.53	39.03	39.14	39.04			
Al ₂ O ₃	0.02	0.01	0.05	0.02			
TiO ₂	0.01	0.01	0.02	0.01			
MgO	44.06	43.34	43.48	42.98			
CaO	0.19	0.17	0.20	0.19			
FeO	18.32	18.39	18.48	18.30			
MnO	0.29	0.32	0.32	0.31			
Na ₂ O	0.02	0.00	0.01	0.00			
K ₂ O	0.02	0.02	0.02	0.02			
Total	101.46	101.29	101.72	100.87			
An, Fo	Fo80.5	Fo80.3	Fo80.1	Fo80.2			

squares fit are shown in Figure 3. Particularly thin samples (20–75 μm) sometimes did not yield useful CO₂ contents because of the presence of interference fringes; such samples are noted in the data tables, and no CO₂ data are reported for them.

[15] The 1σ uncertainties reported in Tables 1–4 for each matrix glass analysis are based on three to six replicate spectra taken on each sample over several days and on several different spots. For the inclusions, for which only one spot could be analyzed, reported errors are

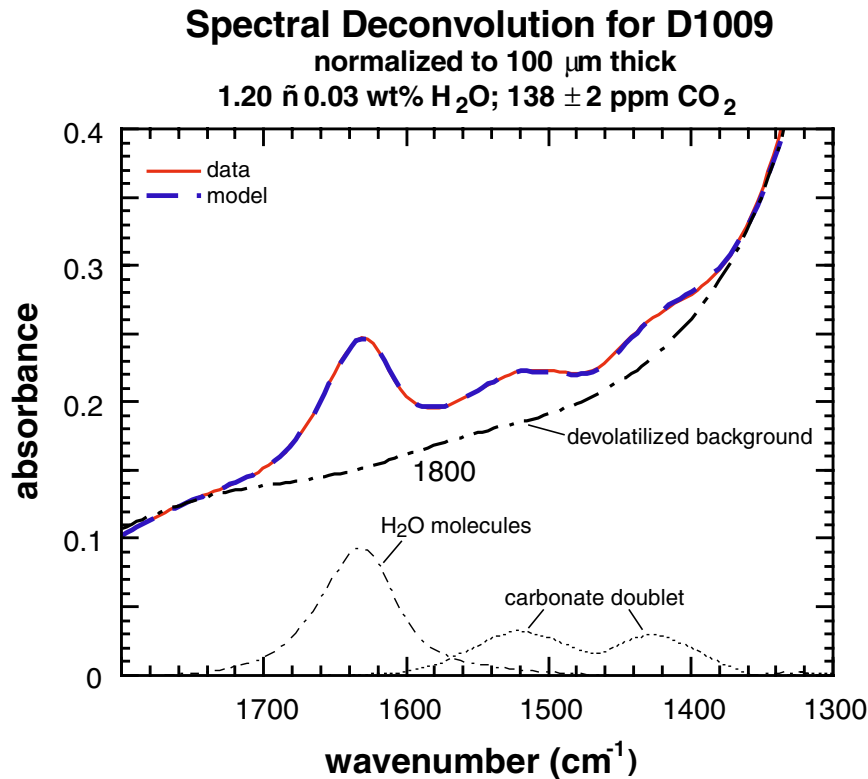


Figure 3. Infrared spectrum in the region of the carbonate doublet for glass from Mariana trough sample D1009. The components that were included in the least squares fit, the background, and the best fit (barely distinguishable from the actual spectrum) are also shown.

based on multiple analyses of the same or overlapping spots. The average relative error based on replicate analyses of the matrix glasses is 6% for total H₂O concentration; the maximum uncertainty is 20%. The average relative error for the dissolved CO₂ content determined in this way is 10%; the maximum uncertainty is 30% for concentrations >30 ppm; lower concentrations are not distinguishable from zero for most samples in the thickness range used here. Note that although several factors affecting the precision of these concentrations are included in the errors based on replicate analyses (e.g., noise in individual spectra, sample heterogeneity), sources of inaccuracy such as errors in molar absorptivity or in the shapes of the spectral components used

to fit the spectra in the region of the carbonate doublet (which could be a particular problem if band and/or background shapes vary from sample to sample or from spectrum to spectrum) contribute uncertainties that are difficult to evaluate. The precision of the FTIR spectrometer was determined by analyzing one spot of a chip of rhyolitic glass from Mono Craters, California (MC84-bb-3b#5) 19 times over the course of this study using the infrared microscope attachment. The resulting relative 1 σ errors in the intensities of the 4500 and 5200 cm⁻¹ bands are ~3%. A basaltic glass from *Michael* [1999] was analyzed four times as a point of interlaboratory comparison. Our data are reported in Table 1 and agree within the uncertainties for both H₂O (0.347 \pm 0.007

wt % in this study versus 0.344 ± 0.020 wt % of *Michael* [1999]) and CO₂ (225 ± 45 ppm in this study versus 268 ± 20 ppm of *Michael* [1999]).

[16] Data for the samples from 18°N were previously published by *Stolper and Newman* [1994]. A second chip for each sample was polished and analyzed in this study using the procedures described above. CO₂ contents were recalculated from the old spectra using the fitting procedure described above; the listed concentrations are averages of the two determinations, except in those cases where the spectra from *Stolper and Newman* [1994] were of significantly lower quality (e.g., owing to large interference fringes or noise). In general, the spectra obtained here are of higher quality owing to the availability of the microscope attachment. The listed H₂O concentrations are also averages of both sets of determinations. The concentrations reported by *Stolper and Newman* [1994] generally agree within error with those reported here; the largest differences are for the two most evolved lavas, ALV 1832-2 and ALV 1833-1, for which the H₂O concentrations given here are higher than of *Stolper and Newman* [1994], and for ALV 1839-21, for which the new CO₂ value is lower.

3.2. Major Elements

[17] The concentrations of major and minor elements in most glass inclusions and their host phenocrysts were determined by wavelength dispersive electron probe microanalysis using Caltech's JEOL 733 Superprobe. The operating conditions were 15-keV accelerating voltage, 10-na beam current, and 10–20 μm beam diameter. Data reduction was done as described by *Armstrong* [1988]. Multiple (two to four) analyses were averaged for each inclusion and host crystal. The VG-2 standard glass [*Jarose-*

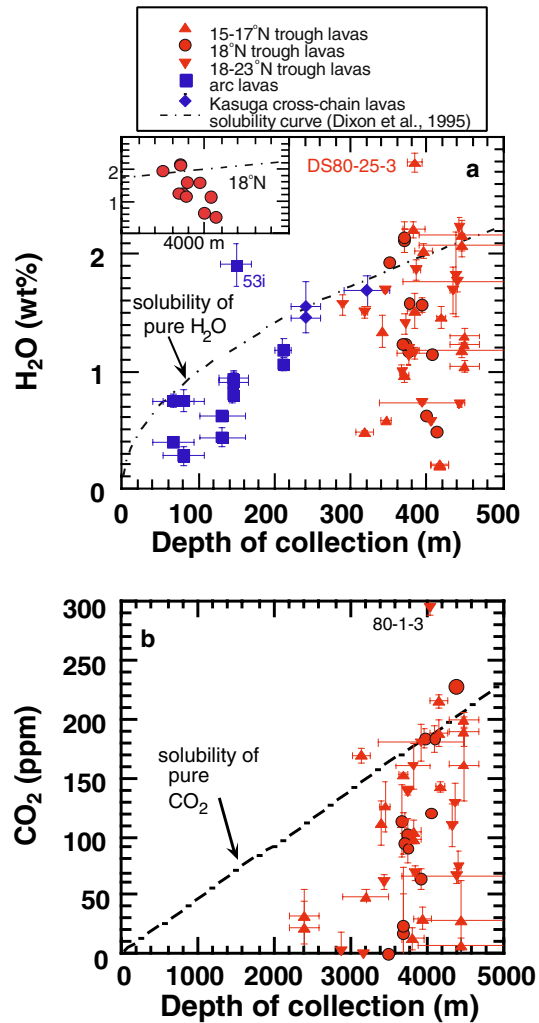


Figure 4. (a) H₂O and (b) CO₂ contents of Mariana trough, arc, and cross-chain volcano glasses (excluding inclusions) versus depth of collection. Uncertainties in depths indicate depth ranges of dredges. Error bars on concentrations in this and other figures are $\pm 1\sigma$. Concentrations of H₂O and CO₂ in melts coexisting with pure H₂O or CO₂ vapor are also shown (calculated as described in footnote a in Table 1 based on the results of *Dixon et al.* [1995]). Glasses from arc and cross-chain lavas are not shown in Figure 4b because they contain no detectable CO₂.



wich *et al.*, 1979] was analyzed several times over the course of this study; its average composition and uncertainties based on the distribution of analyses are given in Table 5.

4. Results and Discussion

[18] Dissolved H₂O and CO₂ contents of host glasses and melt inclusions are given in Tables 1–4. Major element analyses of melt inclusions and their enclosing phenocrysts are reported in Tables 5 and 6. Figures 4–8 show interrelationships between H₂O content, CO₂ content, and other variables. Figure 9 compares the volatile contents of host and inclusion glasses from the Mariana trough and arc with those from other arc and back arc systems and with MORBs.

4.1. Mariana Trough Lavas

4.1.1. Matrix Glasses

[19] The results presented here extend significantly the data presented by *Stolper and Newman* [1994]. The ranges of H₂O contents (0.2–2.8 wt %) and CO₂ contents (from below the detection limit up to ~300 ppm) are significant. The range in H₂O content is comparable with previous results for Mariana trough basalts [*Garcia et al.*, 1979; *Poreda*, 1985; *Stolper and Newman*, 1994] and for other back arc basin basalts [*Muenow et al.*, 1980; *Hochstaedter et al.*, 1990; *Jambon and Zimmermann*, 1990; *Danyushevsky et al.*, 1993], extending from values similar to typical MORB glasses up to much higher values. The range in CO₂ concentration is within the range of previous results for Mariana trough glasses and other infrared measurements of submarine glasses from ridge environments but does not extend to concentrations as high as some seen in mid-ocean ridge environments (Figure 9b) [*Fine and Stolper*, 1985/1986; *Dixon et al.*, 1988; *Stolper and Newman*, 1994; *Pineau and Javoy*, 1994; *Dixon and Stolper*, 1995].

The infrared measurements of dissolved CO₂ content in Mariana trough glasses are much lower than those reported by *Garcia et al.* [1979] using the fusion/quadrupole mass spectrometry technique. This discrepancy has been observed whenever these techniques have been compared [*Fine and Stolper*, 1985/1986; *Dixon et al.*, 1991] and also when results using the fusion/quadrupole mass spectrometry technique have been compared to those from vacuum extraction/manometry [*Des Marais and Moore*, 1984; *Mattey et al.*, 1984]. *Fine and Stolper* [1985/1986] and *Des Marais and Moore* [1984] presented possible explanations for the higher CO₂ concentrations obtained by the fusion/quadrupole mass spectrometry technique, but the issue is not entirely resolved.

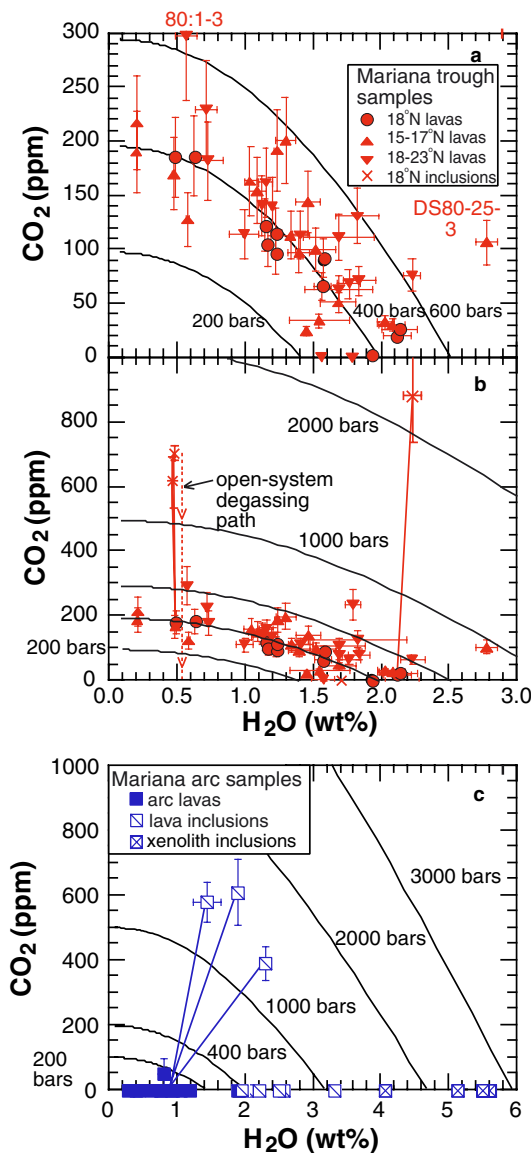
[20] There is no correlation of H₂O or CO₂ content with location along the spreading axis. *Stolper and Newman* [1994] noted a negative correlation between depth of collection and dissolved H₂O content among the 18°N glasses that had not been strongly affected by fractional crystallization; this is clear in the inset in Figure 4a, where these samples are distinguished (the associated positive correlation between CO₂ content and depth is shown less clearly in Figure 4b), but such a correlation is not present among glasses from 15° to 17°N or from 18° to 23°N. The correlation observed for the 18°N glasses could be an artifact of the small number of samples or indicative of a local phenomenon; alternatively, the absence of such a correlation for the other Mariana trough suites, all of which were dredged rather than collected by submersible (as was the case for most of the 18°N suite), could relate to uncertainties in the depth of eruption of the dredged samples.

[21] The key results (Figure 5a) are the negative correlations between the dissolved CO₂ and H₂O contents of the matrix glasses and their



correspondence (albeit with considerable scatter) to the CO₂ + H₂O vapor-saturation curve of tholeiitic liquid at ~400 bars total pressure (i.e., at a pressure corresponding roughly to that on the seafloor where these lavas erupted). Although not yet observed elsewhere among submarine lavas, such a negative correlation is the expected signature of a series of lavas spanning a range of CO₂/H₂O ratio erupted on the seafloor at a single depth under vapor-

saturated conditions. In the case of the Mariana trough magmas the range in initial CO₂/H₂O ratios probably reflects variations in primary magmas in this environment (as previously proposed for the Mariana trough [Stolper and Newman, 1994]), but the observed negative correlation also would result from progressive isobaric fractional crystallization of vapor-saturated magmas [Anderson et al., 1989]. Note that these simple relationships could be obscured if the vapor contained additional components in significant quantities.



[22] As shown in Figure 4, the concentration ranges for both H₂O and CO₂ extend from near the solubility curves of pure H₂O and CO₂ at the depth of eruption (i.e., ~4000 m, corresponding to ~400 bars) down to much lower levels. If the concentration of only one of these two volatiles were known, the relationships observed in Figure 4a or 4b would likely be interpreted as signifying that some magmas erupted significantly undersaturated with respect to vapor; however, the covariation illustrated in Figure 5a demonstrates that this is not the case and emphasizes the importance of having information on all the major volatile

Figure 5. CO₂ versus H₂O contents of glasses from the Mariana arc and back arc system, compared with isobars showing vapor-saturated tholeiitic liquids at various pressures. Vapor-saturated curves based on data from Dixon et al. [1995], calculated as described in footnote a to Table 1. Solid tie lines join melt inclusions and host glasses from the same sample; tie lines between host glasses and melt inclusions with CO₂ contents below detection limit are omitted for clarity. (a) Mariana trough glasses and (b) Mariana trough glasses and glass inclusions in phenocrysts. The dashed line is a representative calculated path for open-system (i.e., fractional) degassing [Anderson et al., 1989; Dixon and Stolper, 1995]. (c) Mariana arc glasses and glass inclusions.

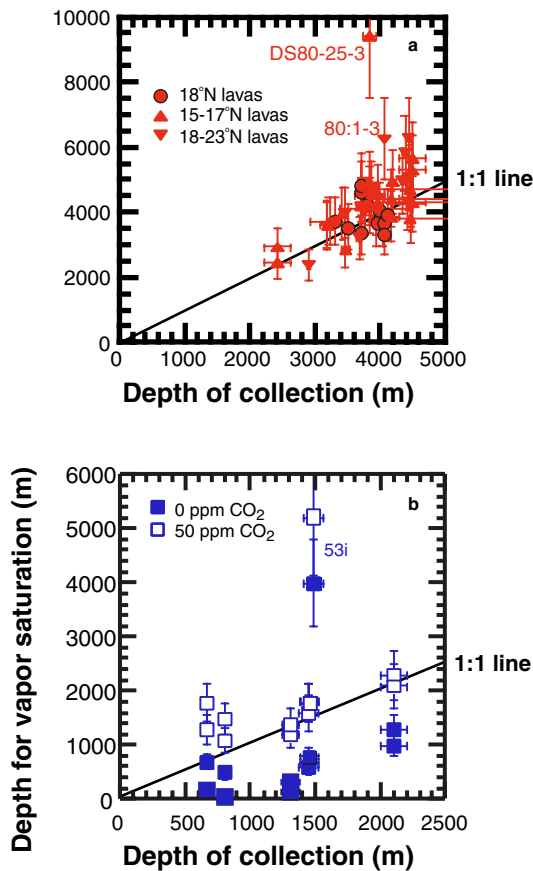
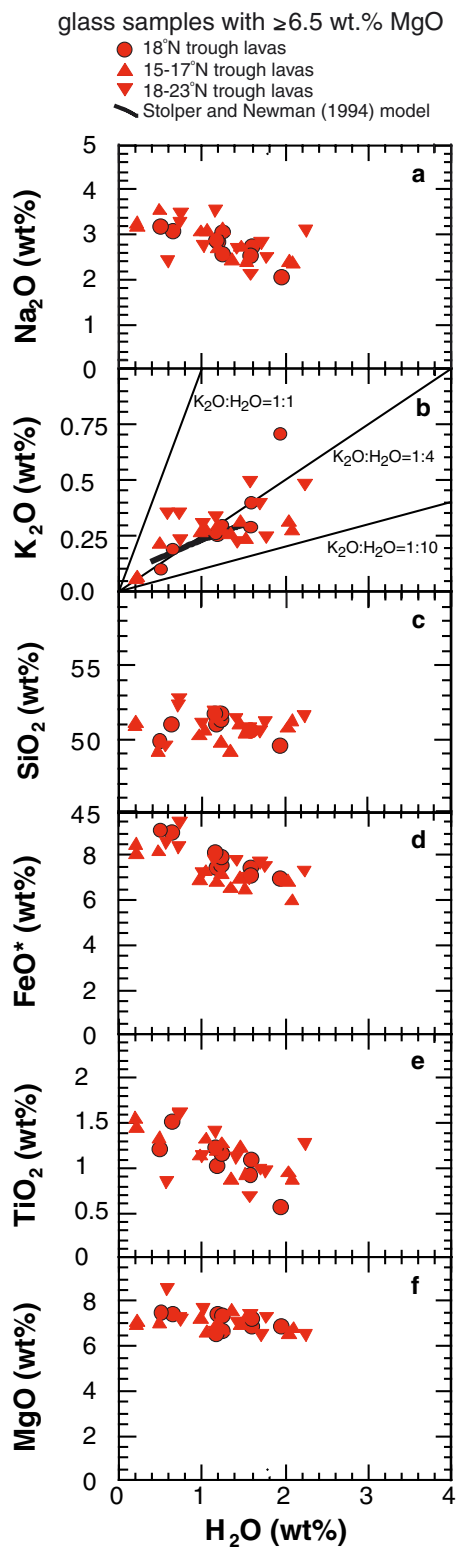


Figure 6. Comparison of depth of collection of submarine lavas and calculated depth of vapor saturation (based on calculated saturation pressure, as described in footnotes a and b to Table 1; error bars on all calculated depths are $\pm 20\%$). (a) Mariana trough glasses and (b) Mariana arc glasses. For the arc glasses, in which CO₂ was in all cases below the detection limit, the depth of vapor saturation was calculated for both 0 and 50 ppm CO₂. Outliers discussed in the text are labeled.

components. There are two significant exceptions to these observations: sample DS80-25-3 from $\sim 16^\circ\text{N}$, which has a much higher H₂O content than the saturation curve (and nonnegligible CO₂), and sample 80:1-3 from $\sim 19^\circ\text{N}$, which has a CO₂ content above the saturation curve. Supersaturation with respect

to CO₂-rich vapor such as that observed for sample 80:1-3 is not uncommon for CO₂-rich magmas on some mid-ocean ridges and has been interpreted as signifying ascent so rapid from a magma chamber that there was insufficient time for degassing [Fine and Stolper, 1985/1986; Dixon *et al.*, 1988; Stolper and Holloway, 1988; Javoy and Pineau, 1991; Pineau and Javoy, 1994]. However, if sample DS80-25-3 was supersaturated with respect to H₂O-rich vapor on eruption (rather than having absorbed water after eruption, which is not suggested by the molecular H₂O to OH ratio [Zhang, 1991; Dixon *et al.*, 1995]), this would be the first example of which we are aware of a H₂O-rich basaltic magma erupting in a significantly supersaturated condition. The overall scatter in Figure 5a and the ~ 20 ppm deviation of several samples above the CO₂ solubility curve in Figure 4b could reflect smaller degrees of supersaturation but are more likely to reflect uncertainties in measured CO₂ contents.

[23] The interpretation of Figure 5a that most trough magmas erupted on the seafloor saturated with CO₂ + H₂O vapor can be explored by using available information on CO₂ and H₂O solubility in basaltic melts to calculate for each analyzed glass composition the pressure at which it would be vapor-saturated and the composition of the vapor. The results of such calculations (explained in footnote a in Table 1) are listed in Table 1. The calculated depth of vapor saturation is then compared to the depth of collection for each sample in Figure 6a. Despite the considerable scatter (and the outliers, DS80-25-3 and 80:1-3, discussed in the preceding paragraph), there is an overall correspondence between collection depth (assumed to equal the eruption depth) and the depth at which the sample is vapor saturated. This supports the hypothesis that these samples were vapor-saturated on eruption.



[24] Models of the degassing of magmas saturated with H₂O + CO₂ vapor [e.g., *Bottinga and Javoy*, 1990a, 1990b; *Dixon and Stolper*, 1995; *Anderson et al.*, 1989] show that because of the much lower solubility of CO₂ than H₂O in most natural liquids at pressures less than a few tens of kilobars, the CO₂/H₂O ratio of the vapor is much greater than that of the coexisting melt. Consequently, during progressive degassing, the CO₂/H₂O ratio of the liquid decreases rapidly. Moreover, these models predict that unless the pressure becomes low enough that the melt is close to saturation with pure H₂O (i.e., it would degas even if no CO₂ were present in the system), the effect of degassing on the H₂O content of the residual melt is negligible. This is illustrated by the dashed, open-system (i.e., fractional) degassing curve shown in Figure 5b. As emphasized by *Stolper and Newman* [1994], this prediction is important because it means that for nearly all of the Mariana trough lavas (and indeed for an even higher percentage of MORBs erupted under submarine conditions, because their H₂O concentrations are at the low end of the range of Mariana trough lavas), even though they are degassing (i.e., “bubbling”) on ascent and eruption on the seafloor, their dissolved H₂O contents are essentially undisturbed and can be used to infer the concentrations of H₂O in primitive, mantle-derived magmas (provided correction can be made for the effects of crystallization). Note, however, that these calculations indicate that the CO₂ contents of submarine glasses will not generally preserve any information about the CO₂ contents of primitive magmas; i.e., they will reflect both

Figure 7. Variation of selected major and minor elements versus H₂O for Mariana trough glasses with $> 6.5\%$ MgO. Figure 7b shows lines for K₂O/H₂O of 1:1, 1.4, and 1:10 following *Danyushevsky et al.* [1993] and the trend (thick solid line) of the volatile-fluxed melting model of *Stolper and Newman* [1994].

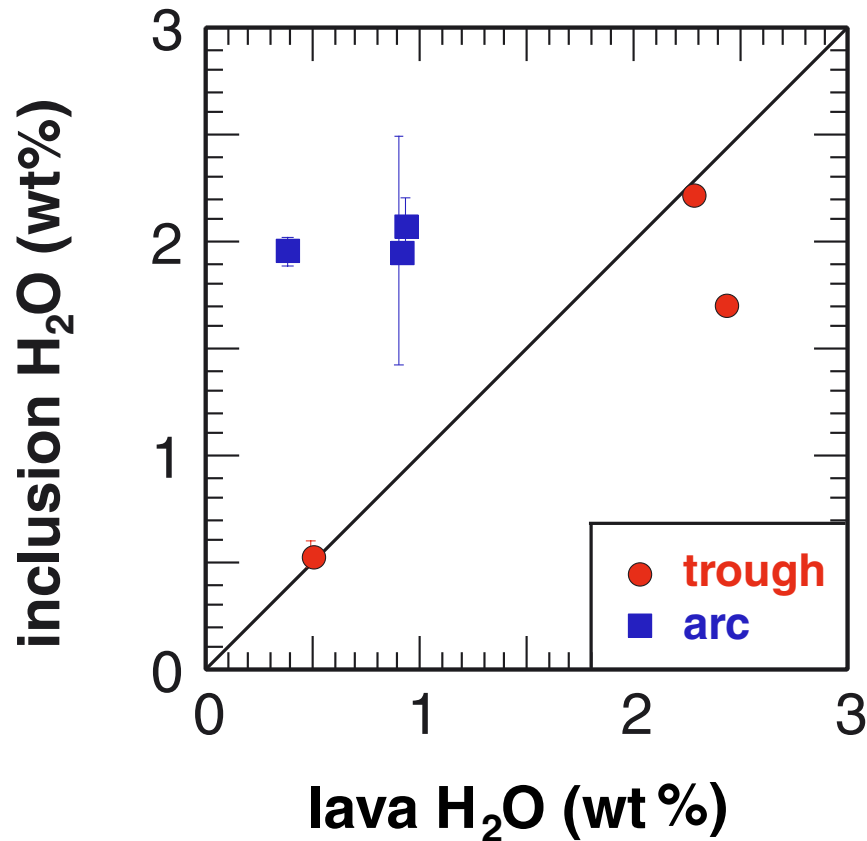


Figure 8. Comparison of H₂O contents of melt inclusions with H₂O contents of the host glasses. For those samples in which more than one inclusion was analyzed, the inclusion H₂O contents are averages, and the error bars span the range of measured water contents.

the CO₂/H₂O ratio of the initial magma and the effects of degassing and the pressure of eruption.

[25] Given the likelihood that the H₂O contents of Mariana trough magmas were essentially unchanged upon eruption, it is possible by restricting the data set to relatively unfractionated samples to examine covariations between the H₂O content and other aspects of chemical composition of mantle-derived magmas and to infer thereby the quantitative role of H₂O in mantle melting. This was the approach used by *Stolper and Newman* [1994] in their study of a much more limited data set from the 18°N

region of the Mariana trough. As shown in Figure 7, the more extensive data set obtained here, covering 900 km along the trough, confirms the strong correlations between H₂O and other elements in primitive Mariana trough glasses observed by *Stolper and Newman* [1994]. The additional data presented here are consistent with their preferred interpretation that the sources of these magmas contain two end members, one H₂O-, K₂O-, and Na₂O-rich and TiO₂-poor (and carrying many of the chemical signatures of arc magmas) and the other similar to a typical source of normal MORB (NMORB) magmas, and that the degree of melting increases with the amount of

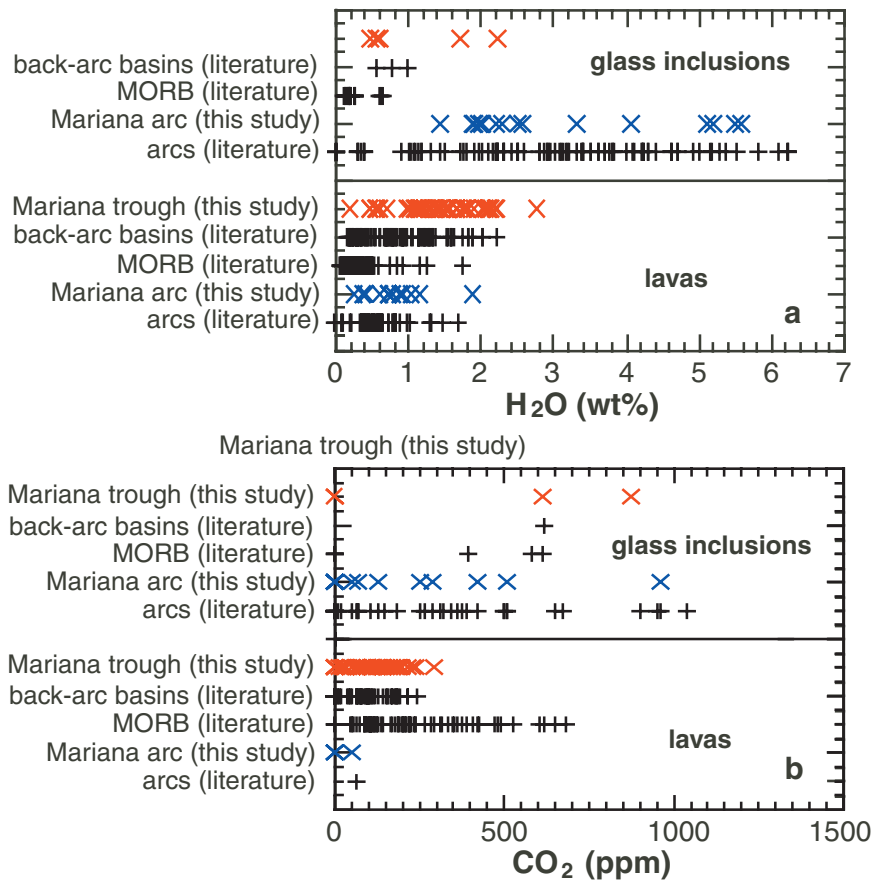


Figure 9. Comparisons of volatile contents of glasses from the Mariana trough and arc (from this study) with data on glasses from arcs, back arc basins, and mid-ocean ridges from Gill [1976], Delaney *et al.* [1978], Garcia *et al.* [1979], Muenow *et al.* [1980], Harris and Anderson [1984], Fine and Stolper [1985/1986], Byers *et al.* [1986], Dixon *et al.* [1988], Hochstaedter *et al.* [1990], Jambon and Zimmermann [1990], Falloon *et al.* [1992], Danyushevsky *et al.* [1993], Metrich *et al.* [1993], Sisson and Layne [1993], Macpherson and Matthey [1994], Pineau and Javoy [1994], Roggensack *et al.* [1996], Sobolev [1996], Sobolev and Chaussidon [1996], Roggensack *et al.* [1997] and data for the East Scotia Sea and the Lau Basin (S. Newman and E. M. Stolper, unpublished data, 1995). (a) Compiled data for H₂O contents for (top) glass inclusions and (bottom) glasses from lavas. (b) Compiled data for CO₂ contents for (top) glass inclusions and (bottom) glasses from lavas.

the H₂O-rich end member in the source. As noted by Danyushevsky *et al.* [1993] and shown in Figure 7b, the Mariana trough samples fall roughly on the same 1:4 K₂O:H₂O trend defined by samples from the Lau Basin [Poreda, 1985; Aggrey *et al.*, 1988; Jambon and Zimmermann, 1990; Vallier *et al.*, 1992], the Sumisu Rift [Hochstaedter *et al.*, 1990], the

Woodlark Basin [Muenow *et al.*, 1990; Danyushevsky *et al.*, 1993], and the Manus Basin [Danyushevsky *et al.*, 1993]. Although Danyushevsky *et al.* [1993] interpreted this group of back arc basins (all of which involve young or immature spreading basins or have overlapping spreading centers) in terms of simple mixing between common subduction compo-



nent and NMORB end members, it can also be explained in terms of the *Stolper and Newman* [1994] model, in which the degree of melting is correlated with the H₂O content of the mixed source. Note finally that the most H₂O-rich of the unfractionated trough glasses, the so-called arc-like samples [*Hawkins et al.*, 1990], have ~2 wt % dissolved H₂O, intermediate between the extremes of recent estimates of the H₂O contents of primitive arc magmas [*Sisson and Layne*, 1993; *Roggensack et al.*, 1997; *Sisson and Bronto*, 1998].

4.1.2. Glass Inclusions

[26] Our results for glass inclusions provide a consistency check on the degassing models discussed above that suggest that H₂O contents of the host glasses preserve preruptive values. Glass inclusions that remain sealed in phenocrysts during eruption do not depressurize and degas along the same path as the enclosing liquid: i.e., whereas the magma achieves a pressure corresponding to the depth of the water into which it erupts, the inclusions follow a path of roughly constant volume during cooling; although this does lead to some depressurization prior to quenching to a glass, the pressure decrease is small compared to that experienced by the host liquid. It is therefore expected that the H₂O contents of leak-tight glass inclusions will be comparable to those of their host glasses, if, as we suggest, the host glasses do not lose significant H₂O on eruption. Note that this behavior is only expected if (1) the initial H₂O content of the melt inclusion and the host melt were the same and neither have evolved significantly by crystallization since entrapment and (2) the lavas erupt at pressures high enough that the magma remains undersaturated with respect to nearly pure H₂O vapor (as described below, this is not the case for the arc lavas included in this study). In contrast to the behavior for H₂O, however, the host glasses are expected to have lost signifi-

cant amounts of CO₂, whereas again the inclusions are expected to preserve preruptive values, and thus we expect that the CO₂ contents of the inclusions will in general exceed those of the matrix glasses.

[27] The H₂O and CO₂ contents of the glass inclusions from the Mariana trough samples are listed in Table 2 and shown in Figures 5b and 8. Four inclusions in olivine in WOK 28-3 were analyzed for H₂O: their average H₂O content (0.53 ± 0.06 wt %) overlaps that of the host glass (0.49 ± 0.01 wt %). Only two of these inclusions were analyzed for CO₂ (as described above, interference fringes prevented accurate measurements for the others): their CO₂ contents (691 ± 28 and 613 ± 78 ppm) are significantly higher than that of the host glass (183 ± 10 ppm). Thus, for this sample, the predicted behavior (much higher CO₂ in the inclusions relative to the host glass but essentially identical H₂O) is observed. The same is observed for the inclusion in plagioclase in ALV 1832-2, where the CO₂ in the inclusion (875 ± 141 ppm) is much higher than that in the host glass (18 ± 5 ppm) but the H₂O contents (2.23 ± 0.07 versus 2.12 ± 0.10 wt %) are indistinguishable. The analyzed inclusion in plagioclase in ALV 1833-1 is connected to the host glass by a capillary, so the fact that its CO₂ is not detectable is not unexpected; the fact that the H₂O content of the inclusion is actually lower than that of the host glass in this case (1.71 ± 0.01 versus 2.14 ± 0.13 wt %) may reflect complications associated with the degassing process or a difference in the composition of trapped melt and the host glass inherited from the time of trapping (see below).

[28] The measurements on the glass inclusions in the Mariana trough samples demonstrate two important results. First, they validate our expectation based on degassing calculations that the H₂O contents of the host glasses are not significantly influenced by the degassing that



takes place on eruption. Second, they demonstrate that Mariana trough magmas, whether H₂O-poor and MORB-like (WOK 28-3) or evolved, H₂O-rich, and somewhat more arc-like (ALV 1832-2), can be rich in CO₂ prior to degassing on eruption. Note that the 600–800 ppm CO₂ concentrations of the glass inclusions represent lower limits to those of primitive mantle magmas, since significant degassing may have occurred prior to trapping of melts in the phenocrysts.

[29] Although the similarity of the H₂O contents of the glass inclusions and host glasses can be explained by their both being samples of magmatic liquid that have not evolved significantly in their H₂O content by degassing or crystallization since the trapping of the inclusion, there are several complicating factors. The most significant of these is that the major element composition of individual Mariana trough (and arc; see below) glass inclusions cannot be simply related to the matrix glass by crystallization of the enclosing phenocrysts or other phenocrysts found in related lavas, so the assumption that the H₂O content of the inclusions and the host melt were ever identical may not be valid. Even the four inclusions from WOK 28-3, although similar to each other, cannot be simply related by crystallization (Table 6). A similar result was obtained by *Lee and Stern* [1998] in their comparison of Mariana arc lavas and glass inclusions in phenocrysts. Based on similar observations on MORBs, *Sobolev* [1996] and *Kent et al.* [1998] concluded that melt inclusions sample a range of liquid compositions that existed at depth prior to their having been blended in magma chambers and/or conduits to produce erupted matrix glasses.

[30] Given the difference in major element composition between the inclusions and host glasses, the surprising result may actually be that the H₂O contents of the inclusions and

host glasses are so similar for the trough samples (Figure 8). One possibility is that the H₂O contents of the inclusions actually differed at the time of trapping (like other aspects of the chemical composition) from that of the current host magma but that the phenocryst hosts act as semipermeable membranes, allowing transport of hydrogen between the melt inside and outside the phenocrysts. *Qin et al.* [1992] discussed the factors influencing diffusive reequilibration of chemical components between melt inclusions and host magma through the host mineral; on the basis of their calculations the minimum reequilibration time for the trough melt inclusions can be estimated to be of the order of 10¹–10³ years, depending on the choice of transport and solubility properties for water in olivine [*Qin et al.*, 1992, and references therein]. These timescales are not unreasonable for magma chamber residence times, so even if the “as-trapped” H₂O contents of the inclusions differed from the current host glass, it may not be surprising that the H₂O contents of the inclusions so closely match the H₂O contents of the host glasses since they could have equilibrated with them diffusively through the phenocryst host during residence in a magma chamber prior to eruption. Note that CO₂ exchange across olivine phenocrysts is not expected because CO₂ has significantly smaller partition and diffusion coefficients than mobile H-bearing species [*Tingle et al.*, 1988; *Watson*, 1991; *Qin et al.*, 1992, and references therein].

4.1.3. Crystallization Depths

[31] Assuming the glass inclusions reflect the CO₂ and H₂O contents of vapor-saturated melts at the time of entrapment, it is possible to calculate for each inclusion the pressure at which this entrapment took place (Table 2); if the melt was undersaturated with respect to vapor at the time of entrapment, the pressure calculated assuming vapor saturation is a lower



limit. The glass inclusion in plagioclase from ALV 1832-2 indicates saturation with respect to a mixed H₂O–CO₂ (25 mole % H₂O) vapor phase at ~2.5 kbar. The pressure at the depth of collection was ~0.4 kbar; the additional pressure of ~2100 bars would require crystallization of the plagioclase at ~6–7 km below the seafloor. For the most CO₂-rich melt inclusion from olivine in WOK 28-3 (in OL1) this calculation yields a pressure of ~1.4 kbar (with 2 mole % H₂O in the vapor), corresponding to a depth of ~3 km below the seafloor. This value is similar to the depth of 2.7 km below the seafloor determined for the depth for saturation with CO₂ of the most supersaturated glasses from the Juan de Fuca Ridge [Dixon *et al.*, 1988], in agreement with seismic evidence for the magma chamber there [Morton *et al.*, 1987], although deeper than the 0.8–2.0 km depth inferred for the base of a magma sill at the fast spreading southern East Pacific Rise [Hoofst *et al.*, 1997]. Although subject to considerable uncertainties, especially given the possibility of exchange of H₂O across the phenocrysts, these calculations are consistent with phenocryst crystallization in crustal or shallow upper mantle environments.

4.2. Mariana Arc Lavas

[32] Matrix glasses dredged from submarine portions of the Mariana arc span a range of H₂O contents similar to samples from the Mariana trough: i.e., 0.3–1.9 wt % (Table 3). However, the depths of collection of these arc lavas are significantly lower than those of the trough lavas (~500–2000 m for the arc samples, compared to ~3500–4500 m for the trough samples). Consequently, for magmas with H₂O contents higher than 0.7–1.4 wt % H₂O the H₂O content of the liquid phase would have been affected by degassing on eruption provided there was sufficient time for nucleation and growth of bubbles. As expected for low-pressure degassing of H₂O-rich, CO₂-poor

magmas [Dixon and Stolper, 1995], the H₂O contents of the arc glasses are positively correlated with depth of collection, and, with a single exception, the H₂O content versus depth trend of the arc samples parallels but is somewhat lower than the trend for the solubility of pure H₂O (Figure 4a). All of the host glasses have CO₂ contents at or below the detection limit, also consistent with extensive, low-pressure degassing due to eruption on the seafloor under vapor-saturated conditions: i.e., at the low pressures of eruption, even if the melts were saturated with pure CO₂ vapor, the CO₂ concentrations of the glasses would only be 25–75 ppm; however, given the H₂O contents of the glasses, the CO₂ contents of vapor-saturated melts at the depths of collection would be ~10–50 ppm. In detail, the data for the host glasses are consistent with the magmas initially having had higher H₂O contents (as indicated by the undegassed glass inclusions; see below), and then having degassed on eruption to a H₂O content controlled by saturation with a vapor with 25–100% H₂O. As shown in Figure 6b, if all of these arc glasses are assumed to contain 50 ppm CO₂, there is a reasonable correspondence between the depth of vapor saturation and the actual depth of collection.

[33] As described in the previous section in connection with the trough lavas, one way of establishing whether degassing of H₂O occurred on eruption is to compare the water contents of melt inclusions in phenocrysts and their host glasses. As shown in Figure 8, in contrast to the trough samples, for the arc samples the H₂O contents of the host glasses are systematically lower than those of the glass inclusions. This offers strong evidence, particularly in view of the contrasting behavior of the trough glasses, that H₂O contents of the arc liquid portions of the arc magmas were influenced by degassing on eruption because of the low pressures of eruption. The H₂O contents of



the intermediate to basic glass inclusions (1.4–3.3 wt % H₂O; see Table 4) therefore provide the best approximation available from this work of the H₂O contents of mantle-derived Mariana arc magmas. Although these glasses all represent liquids that have experienced some crystal fractionation and enrichment of H₂O relative to “primary” magmas, the fact that the relatively primitive, clinopyroxene (cpx)-hosted inclusion from sample 38-2 with 7.25 wt % MgO (consistent with ~10% olivine fractionation or 30% high-Ca pyroxene fractionation from a melt with 10% MgO) has 3.3 wt % H₂O indicates that the upper end of this range has not been dramatically influenced by this effect.

[34] The values inferred here for primitive Mariana arc magmas are similar to the arc-like end of the array defined by primitive Mariana trough samples (~2 wt % H₂O; Figure 7), and they are in the range of previously reported measurements and estimates for arc magmas (which range from values of 0.2–0.4% H₂O for glass inclusions inferred to have been produced by a significant component of decompression melting beneath arcs [Sisson and Bronto, 1998] to values as high as 6% H₂O [e.g., Sisson and Grove, 1993; Sisson and Layne, 1993; Roggensack et al., 1997]). Most other studies of glass inclusions in phenocrysts in arc lavas have yielded H₂O contents similar to the values inferred here for the Mariana arc and for the arc-like end of the Mariana trough lavas: for example, 1.3–3.4 wt % for Fuego volcano [Harris and Anderson, 1984], 1.4–2.6 wt % for Kamchatka [Sobolev and Chaussidon, 1996], and 2.0–3.8 wt % for Rabaul [Roggensack et al., 1996]. The values from glass inclusions from this and other studies could represent lower limits, degassed from even more H₂O-rich magmas, but the preservation of high CO₂ contents (~400–600 ppm) in several inclusions with 1.4–2.3 wt % H₂O (Figure 5c) from the North Hiyoshi

seamount argues against this, at least for these samples, because the calculated minimum pressures of vapor-saturated entrapment of these CO₂-bearing inclusions, 1.3–1.6 kbar, are sufficiently high that negligible amounts of H₂O would partition into a vapor phase under these conditions. This argument also applies to CO₂-rich glass inclusions in olivine from Galunggung (Indonesia), Rabaul (Papua New Guinea), and Cerro Negro (Nicaragua) [Roggensack et al., 1996, 1997; Sisson and Bronto, 1998].

[35] It may be significant that only inclusions from a shoshonitic North Hiyoshi sample have high CO₂ contents, perhaps reflective of a systematic difference between sources of shoshonitic magmas and those of more typical Mariana arc magmas; note that the only shoshonitic magmas in our sample set come from where the back arc spreading center is propagating into the arc, and thus it is possible that the high CO₂ contents of these inclusions reflect a contribution from “fresh” mantle wedge material not depleted in CO₂ by previous extraction of arc or back arc basalts. On the other hand, the 400–600 ppm CO₂ measured in these inclusions is similar to values in glass inclusions from nonshoshonitic lavas from other arcs [Roggensack et al., 1996, 1997; Sisson and Bronto, 1998], perhaps suggesting that these levels of CO₂ (which are only lower limits) are typical of undegassed arc magmas and that CO₂, although difficult to characterize in most arc magmas since they are nearly fully degassed on eruption, could be a significant volatile component in arc systems.

[36] The single exception to the overall trends for the arc lavas is rhyolitic sample 53i from the North Hiyoshi seamount; with 1.9 wt % H₂O, this sample has probably been affected by low temperature hydration given its high ratio of H₂O molecules to OH groups (5.6



versus 0.6 for unaltered experimental rhyolite glass with similar total H₂O content [*Silver*, 1988]); such an enhancement in molecular H₂O to OH during hydration of rhyolitic glass has been observed experimentally by *Zhang et al.* [1991].

4.2.1. Glass Inclusions in the Agrigan Cumulate Xenolith

[37] The melt inclusions in olivine grains from the cumulate xenolith from Agrigan have much higher H₂O contents (4.1–5.6 wt %) than those from the glass inclusions in the arc lavas. Although similarly high and even higher values were reported for basaltic andesite and basaltic melt inclusions in olivine phenocrysts from Fuego volcano (Guatemala) by *Sisson and Layne* [1993] (1.0–6.2 wt % H₂O) and Cerro Negro volcano (Nicaragua) by *Roggen-sack et al.* [1997] (1.1–6.1 wt % H₂O), the evolution of residual liquids and textures in cumulates can lead to compositions far removed from primitive liquids, so the significance of the high water contents in the olivine-hosted inclusions from Agrigan for estimates of the volatile contents of more primitive liquids is not clear. Although these results clearly demonstrate the existence of high-H₂O liquids in the Mariana arc system, we consider the lower values from the inclusions in arc lavas to be more representative of the volatile contents of primitive magmas from the Mariana arc. Note in particular that the major element compositions of the inclusions from the xenolith indicate that they are far removed from primary compositions (e.g., their MgO contents are 2–4 wt %), and extensive crystallization could have increased H₂O contents well above their levels in primitive liquids.

4.2.2. Crystallization Depths

[38] Assuming that the glass inclusions from the arc lavas reflect the CO₂ and H₂O contents

of vapor-saturated melts at the time of entrapment, it is possible, as described above, to calculate for each inclusion the minimum pressure at which entrapment took place (Table 4). Calculated pressures for the CO₂-bearing inclusions from the shoshonitic North Hiyoshi lava are 1.3–1.6 kbar, corresponding to depths of ~4 km below the seafloor; calculated vapor compositions are ~15–40% H₂O. The calculated pressure for the one arc-lava inclusion with no detectable CO₂ (the inclusion in PLAG2 in the 29:2-2 Daikoku lava) assumes saturation with respect to pure H₂O vapor and yields a pressure of 0.5 kbar, corresponding to a depth of ~0.7 km below the local seafloor. These depths for inclusions from the submarine arc lavas overlap those inferred from melt inclusions from the trough lavas. For the Agrigan xenolith, calculated pressures are 1.6–2.6 kbar, corresponding to crustal depths of 5–8 km. This calculated depth is compatible with the ≤ 7 km depth estimated by *Stern* [1979] based on the petrology of Agrigan xenoliths.

4.3. Cross-Chain Seamount Lavas

[39] The three basaltic lavas from the cross-chain seamounts have a narrow range of H₂O contents (1.4–1.7 wt % H₂O). Since these samples are vesicular, they were vapor-saturated on eruption. However, the vapor compositions must have been nearly pure H₂O since these samples fall within error on the H₂O solubility curve for basaltic liquids (i.e., they have precisely the amount of dissolved H₂O for a melt coexisting with pure H₂O at the depth of collection; the calculated amounts of CO₂ in melts that would be required for these samples to be vapor saturated at the depths of collection are <23 ppm; see Table 3). This inference is consistent with the fact that the measured CO₂ contents are below the detection limit (<~30 ppm for these samples). Since the inferred vapor phase is



nearly pure H₂O, the H₂O contents of the primitive cross-chain magmas must have been higher than the 1.4–1.7 wt % we have measured.

5. Conclusions

[40] 1. We have extended considerably the database for H₂O and CO₂ contents of submarine glasses from the Mariana trough; the new data set comprises primarily measurements on pillow rim glasses but also includes inclusions in phenocryst phases. Excluding the glass inclusions, these glasses show a wide range of both H₂O and CO₂ concentrations (0.2–2.8 wt % H₂O; 0–300 ppm CO₂) that are negatively correlated. The negative correlation is a consequence of saturation of the erupting liquid with a CO₂–H₂O vapor at the pressure of eruption (~400 bars for these samples), with the vapor ranging from nearly pure CO₂ at the CO₂-rich end of the glass array to nearly pure H₂O at the H₂O-rich end. The H₂O contents of glass inclusions in phenocrysts are similar to those of the host glasses for these trough samples, but the CO₂ contents (up to 875 ppm) can be considerably higher; this confirms expectations based on simple degassing models that degassing of these magmas on ascent and eruption leads to significant loss of CO₂ (thereby masking pre-eruptive CO₂ contents) but preserves pre-eruptive H₂O contents. The depth of crystallization of the inclusion-bearing phenocrysts was at least 3–7 km below the seafloor. The range in H₂O contents of the trough magmas and the correlations between H₂O contents and other aspects of the chemical and isotopic compositions of these samples are consistent with the model of *Stolper and Newman* [1994] that compositional variations among primitive magmas in this suite result from melting of mixtures of an H₂O-poor NMORB-type source region component with an H₂O-rich slab-derived component, where

the amount of melting is a function of the H₂O content of the mixture. The H₂O contents of primitive Mariana trough magmas richest in the slab-derived component (i.e., most arc-like) are ~2 wt %.

[41] 2. We measured H₂O and CO₂ contents of submarine glasses dredged from the Mariana arc and of glass inclusions in phenocrysts from these samples and in olivines from a composite gabbro + anorthosite xenolith from Agrigan (a Mariana arc island). The submarine glasses contain 0.3–1.9 wt % H₂O and ≤50 ppm CO₂. Water depths were low enough relative to the H₂O content of the liquid phase in these magmas that degassing on ascent and eruption led to loss of both H₂O and CO₂, in contrast to the Mariana trough lavas, which erupted at significantly higher water depths and thus only degassed CO₂ in significant quantities; as a result, H₂O contents are positively correlated with water depth in these samples. Glass inclusions from the arc lavas contain more H₂O (1.4–3.3%) than their host glasses, as expected given the loss of H₂O from the host liquids on ascent and eruption. The inclusion with 3.3% H₂O has the most primitive chemical composition (>7% MgO). We conclude that primitive arc magmas in the Mariana arc contain ~1–3% H₂O. CO₂ is below the detection limit in the glass inclusions, except for inclusions in a shoshonitic lava from North Hiyoshi seamount, which contain 400–600 ppm CO₂. Since the back arc spreading regime intersects the arc near North Hiyoshi, this could indicate the presence of CO₂-rich mantle wedge material under the arc at this location, in contrast to mantle wedge material elsewhere under the arc, which may have previously lost its CO₂ during arc and/or back arc magma generation. The glass inclusions from the Agrigan xenolith are highly evolved relative to those in the arc lavas, and they contain 4–6% H₂O and CO₂ below detection limit. Although demonstrating the existence of H₂O-rich arc mag-



mas in the Marianas, these values may not be representative of primitive magmas. Volatile contents of melt inclusions from arc lavas and the xenolith imply minimum depths of crystallization (~1–8 km) similar to those in the trough.

[42] 3. Submarine glasses from the Kasuga cross-arc seamounts in the Marianas contain no detectable CO₂ and 1.4–1.7% H₂O. They plot on the saturation curve for nearly pure H₂O-vapor at the depth of eruption. This signifies loss of H₂O by degassing during ascent and eruption and indicates preeruptive H₂O contents of $\leq \sim 1.5\%$.

Acknowledgments

[43] We thank James Hawkins of Scripps Institution of Oceanography for providing the *Alvin* and WOK Mariana trough samples. Help with electron microprobe analyses was generously provided by Paul Carpenter. This work was supported by NSF grant EAR-9117588. Division of Geological and Planetary Sciences contribution 8691.

References

- Aggrey, K. E., D. W. Muenow, and R. Batiza, Volatile abundances in basaltic glasses from seamounts flanking the East Pacific Rise at 21°N and 12–14°N, *Geochim. Cosmochim. Acta*, **52**, 2115–2119, 1988.
- Anderson, A. T., Jr., Hourglass inclusions: Theory and application to the Bishop rhyolitic tuff, *Am. Mineral.*, **76**, 530–547, 1991.
- Anderson, A. T., Jr., S. Newman, S. N. Williams, T. H. Druitt, C. Skirius, and E. Stolper, H₂O, CO₂, Cl, and gas in Plinian and ash-flow Bishop rhyolite, *Geology*, **17**, 221–225, 1989.
- Armstrong, J. T., Quantitative analysis of silicate and oxide minerals; comparison of Monte Carlo, ZAF and $\varphi(\rho z)$ procedures, in *Microbeam Analysis*, pp. 239–246, edited by D. E. Newbury, San Francisco Press, San Francisco, Calif., 1988.
- Baker, M. B., T. L. Grove, and R. Price, Primitive basalts and andesites from the Mt. Shasta region, N. California: Products of varying melt fraction and water content, *Contrib. Mineral. Petrol.*, **118**, 111–129, 1994.
- Blank, J. G., E. M. Stolper, and M. R. Carroll, Solubilities of carbon dioxide and water in rhyolitic melt at 850°C and 750 bars, *Earth Planet. Sci. Lett.*, **119**, 27–36, 1993.
- Bloomer, S. H., R. J. Stern, E. Fisk, and C. H. Geschwind, Shoshonitic volcanism in the northern Mariana Arc, 1, Mineralogic and major and trace element characteristics, *J. Geophys. Res.*, **94**, 4469–4496, 1989a.
- Bloomer, S. H., R. J. Stern, and N. C. Smoot, Physical volcanology of the submarine Mariana and Volcano arcs, *Bull. Volcanol.*, **51**, 210–224, 1989b.
- Bottinga, Y., and M. Javoy, Mid-ocean ridge basalt degassing: Bubble nucleation, *J. Geophys. Res.*, **95**, 5125–5131, 1990a.
- Bottinga, Y., and M. Javoy, MORB degassing: Bubble growth and ascent, *Chem. Geol.*, **81**, 255–270, 1990b.
- Byers, C. D., M. O. Garcia, and D. W. Muenow, Volatiles in basaltic glasses from the East Pacific Rise at 21°N: Implications for MORB sources and submarine lava flow morphology, *Earth Planet. Sci. Lett.*, **79**, 9–20, 1986.
- Danyushevsky, L. V., T. J. Falloon, A. V. Sobolev, A. J. Crawford, M. Carroll, and R. C. Price, The H₂O content of basalt glasses from southwest Pacific back arc basins, *Earth Planet. Sci. Lett.*, **117**, 347–362, 1993.
- Danyushevsky, L. V., A. V. Sobolev, and L. V. Dmitriev, Estimation of the pressure of crystallization and H₂O content of MORB and BABB glasses Calibration of an empirical technique, *Mineral. Petrol.*, **57**, 185–204, 1996.
- Delaney, J. R., D. W. Muenow, and D. G. Graham, Abundance and distribution of water, carbon and sulfur in glassy rims of submarine pillow basalts, *Geochim. Cosmochim. Acta*, **42**, 581–594, 1978.
- Des Marais, D. J., and J. G. Moore, Carbon and its isotopes in mid-oceanic basaltic glasses, *Earth Planet. Sci. Lett.*, **69**, 43–57, 1984.
- Devine, J. D., and H. Sigurdsson, Petrology and eruption styles of Kick'em-Jenny submarine volcano, Lesser Antilles island arc, *J. Volcanol. Geotherm. Res.*, **69**, 35–58, 1995.
- Dixon, J. E., and E. M. Stolper, An experimental study of water and carbon dioxide solubilities in mid-ocean ridge basaltic liquids, Part II, Applications to degassing, *J. Petrol.*, **36**, 1633–1646, 1995.
- Dixon, J. E., E. Stolper, and J. R. Delaney, Infrared spectroscopic measurements of CO₂ and H₂O in Juan de Fuca ridge basaltic glasses, *Earth Planet. Sci. Lett.*, **90**, 87–104, 1988.
- Dixon, J. E., D. A. Clague, and E. M. Stolper, Degassing history of water, sulfur, and carbon in submarine lavas from Kilauea volcano, Hawaii, *J. Geol.*, **99**, 371–394, 1991.
- Dixon, J. E., E. M. Stolper, and J. R. Holloway, An



- experimental study of water and carbon dioxide solubilities in mid-ocean ridge basaltic liquids, Part I, Calibration and solubility models, *J. Petrol.*, *36*, 1607–1631, 1995.
- Dobson, P. F., S. Epstein, and E. M. Stolper, Hydrogen isotope fractionation between coexisting vapor and silicate glasses and melts at low pressure, *Geochim. Cosmochim. Acta*, *53*, 223–230, 1989.
- Falloon, T. J., A. Malahoff, L. P. Zonenshain, and Y. Bogdanov, Petrology and geochemistry of back arc basin basalts from Lau Basin spreading ridges, *Mineral. Petrol.*, *47*, 1–35, 1992.
- Fine, G., and E. Stolper, Dissolved carbon dioxide in basaltic glasses: Concentrations and speciation, *Earth Planet. Sci. Lett.*, *76*, 263–278, 1985/1986.
- Fryer, P., J. B. Gill, and M. C. Jackson, Volcanologic and tectonic evolution of the Kasuga seamounts, northern Mariana trough: *Alvin* submersible investigations, *J. Volcanol. Geotherm. Res.*, *79*, 277–311, 1997.
- Garcia, M. O., N. W. K. Liu, and D. W. Muenow, Volatiles in submarine volcanic rocks from the Mariana Island arc and trough, *Geochim. Cosmochim. Acta*, *43*, 305–312, 1979.
- Gardner, J. E., M. Rutherford, S. Carey, and H. Sigurdson, Experimental constraints on pre-eruptive water contents and changing magma storage prior to explosive eruptions of Mount St. Helens volcano, *Bull. Volcanol.*, *57*, 1–17, 1995.
- Gill, J. B., Compositions and age of Lau Basin and ridge volcanic rocks: Implications for evolution of an interarc basin and remnant arc, *Bull., Geol. Soc. Am.*, *87*, 1384–1395, 1976.
- Gribble, R. F., R. J. Stern, S. H. Bloomer, D. Stuben, T. O’Hearn, and S. Newman, MORB mantle and subduction components interact to generate basalts in the southern Mariana trough back arc basin, *Geochim. Cosmochim. Acta*, *60*, 2153–2166, 1996.
- Gribble, R. F., R. J. Stern, S. Newman, S. H. Bloomer, and T. O’Hearn, Chemical and isotopic composition of lavas from the northern Mariana trough: Implications for magmagenesis in backarc basins, *J. Petrol.*, *39*, 125–154, 1998.
- Harris, D. M., and A. T. Anderson Jr., Volatiles H₂O, CO₂ and Cl in a subduction related basalt, *Contrib. Mineral. Petrol.*, *87*, 120–128, 1984.
- Hauri, E., Water in the Hawaiian plume: Where did it come from and where did it go?, *Eos Trans. AGU*, *79(17)*, Spring Meet. Suppl., S209, 1998.
- Hawkins, J. W., and J. T. Melchior, Petrology of Mariana trough and Lau basin basalts, *J. Geophys. Res.*, *90*, 11,431–11,468, 1985.
- Hawkins, J. W., P. F. Lonsdale, J. D. Macdougall, and A. M. Volpe, Petrology of the axial ridge of the Mariana Trough backarc spreading center, *Earth Planet. Sci. Lett.*, *100*, 226–250, 1990.
- Hochstaedter, A. G., J. B. Gill, M. Kusakabe, S. Newman, M. Pringle, B. Taylor, and P. Fryer, Volcanism in the Sumisu Rift, 1, Major element, volatile, and stable isotope geochemistry, *Earth Planet. Sci. Lett.*, *100*, 179–194, 1990.
- Holloway, J. R., Fugacity and activity of molecular species in supercritical fluids, in *Thermodynamics and Geology*, edited by D. J. Fraser, pp. 167–181, D. Reidel, Norwell, Mass., 1977.
- Hooft, E. E. E., R. S. Detrick, and G. M. Kent, Seismic structure and indicators of magma budget along the Southern East Pacific Rise, *J. Geophys. Res.*, *102*, 27,319–27,340, 1997.
- Ikeda, Y., K. Nagao, R. J. Stern, M. Yuasa, and S. Newman, Noble gases in pillow basalt glasses from the northern Mariana Trough back arc basin, *The Island Arc*, *7*, 471–478, 1998.
- Jackson, M. C., Petrology and petrogenesis of recent submarine volcanoes from the northern Mariana arc and back arc basin, Ph.D. thesis, Univ. of Hawaii, Honolulu, 1989.
- Jambon, A., and J. L. Zimmermann, Water in oceanic basalts: Evidence for dehydration of recycled crust, *Earth Planet. Sci. Lett.*, *101*, 323–331, 1990.
- Jarosewich, E. J., J. A. Nelen, and J. A. Norberg, Reference samples for electron microprobe analysis, *Smithsonian Contrib. Earth Sci.*, *22*, 68–72, 1979.
- Javoy, M., and F. Pineau, The volatiles record of a “popping” rock from the Mid-Atlantic Ridge at 14° N: Chemical and isotopic composition of gas trapped in the vesicles, *Earth Planet. Sci. Lett.*, *107*, 598–611, 1991.
- Jendrzewski, N., M. Javoy, and T. Trull, Mésures quantitatives de carbone et d’eau dans les verres basaltiques naturels par spectroscopie infrarouge, Partie I, Le carbone, *C. R. Acad. Sci. Paris*, *322*, 645–652, 1996a.
- Jendrzewski, N., M. Javoy, and T. Trull, Mésures quantitatives de carbone et d’eau dans les verres basaltiques naturels par spectroscopie infrarouge, Partie II, L’eau, *C. R. Acad. Sci. Paris*, *322*, 735–742, 1996b.
- Kent, A. J. R., E. M. Stolper, J. Woodhead, I. D. Hutchison, and F. Francis, Using glass inclusions to investigate a heterogeneous mantle: An example from N- and EMORB-like lavas from Baffin Island, *Mineral Mag.*, *62A*, 765–766, 1998.
- Lee, J., and R. J. Stern, Glass inclusions in Mariana Arc phenocrysts: A new perspective on magmatic evolution in a typical intra-oceanic arc, *J. Geol.*, *106*, 19–33, 1998.



- Lin, P.-N., R. J. Stern, and S. H. Bloomer, Shoshonitic volcanism in the northern Mariana Arc, 2, Large-ion lithophile and rare earth element abundances: Evidence for the source of incompatible element enrichments in intraoceanic arcs, *J. Geophys. Res.*, *94*, 4497–4514, 1989.
- Macpherson, C., and D. Matthey, Carbon isotope variations of CO₂ in Central Lau Basin basalts and ferrobasalts, *Earth Planet. Sci. Lett.*, *121*, 263–276, 1994.
- Martinez, F., P. Fryer, N. A. Baker, and T. Yamazaki, Evolution of back arc rifting: Mariana trough, 20°–24°N, *J. Geophys. Res.*, *100*, 3807–3827, 1995.
- Matthey, D. P., R. H. Carr, I. P. Wright, and C. T. Pillinger, Carbon isotopes in submarine basalts, *Earth Planet. Sci. Lett.*, *70*, 196–206, 1984.
- Merzbacher, C., and D. H. Eggler, A magmatic geothermometer: Application to Mount St. Helens and other dacitic magmas, *Geology*, *12*, 587–590, 1984.
- Metrich, N., R. Clocchiatti, M. Mosbah, and M. Chaussidon, The 1989–1990 activity of Etna magma mingling and ascent of H₂O-Cl-S-rich basaltic magma: Evidence from melt inclusions, *J. Volcanol. Geotherm. Res.*, *59*, 131–144, 1993.
- Michael, P. J., Implications for magmatic processes at Ontong Java Plateau from volatile and major element contents of Cretaceous basalt glasses (on-line), *Geochem. Geophys. Geosyst.*, vol. 1, Paper number 1999GC000017, Dec. 16, 1999.
- Morton, J. L., N. H. Sleep, W. R. Normark, and D. H. Tompkins, Structure of the southern Juan de Fuca Ridge from seismic reflection records, *J. Geophys. Res.*, *92*, 11,315–11,326, 1987.
- Muenow, D. W., N. W. K. Liu, M. O. Garcia, and A. D. Saunders, Volatiles in submarine volcanic rocks from the spreading axis of the East Scotia Sea back arc basin, *Earth Planet. Sci. Lett.*, *47*, 272–278, 1980.
- Muenow, D. W., M. O. Garcia, K. E. Aggrey, U. Bednarz, and H. U. Schmincke, Volatiles in submarine glasses as a discriminant of tectonic origin: Application to the Troodos ophiolite, *Nature*, *343*, 159–161, 1990.
- Newman, S., E. M. Stolper, and S. Epstein, Measurement of water in rhyolitic glasses—Calibration of an infrared spectroscopic technique, *Am. Mineral.*, *71*, 1527–1541, 1986.
- Pandya, N., D. W. Muenow, and S. K. Sharma, The effect of bulk composition on the speciation of water in submarine volcanic glasses, *Geochim. Cosmochim. Acta*, *56*, 1875–1883, 1992.
- Pineau, F., and M. Javoy, Strong degassing at ridge crests: The behavior of dissolved carbon and water in basalt glasses at 14°N, Mid-Atlantic Ridge, *Earth Planet. Sci. Lett.*, *123*, 179–198, 1994.
- Poreda, R., Helium-3 and deuterium in back arc basalts: Lau Basin and the Mariana Trough, *Earth Planet. Sci. Lett.*, *73*, 244–254, 1985.
- Qin, Z., F. Lu, and A. T. Anderson Jr., Diffusive reequilibration of melt and fluid inclusions, *Am. Mineral.*, *77*, 565–576, 1992.
- Roggensack, K., S. N. Williams, S. J. Schaefer, and R. A. Parnell Jr., Volatiles from the 1994 eruptions of Rabaul: Understanding large caldera systems, *Science*, *273*, 490–493, 1996.
- Roggensack, K., R. L. Hervig, S. B. McKnight, and S. N. Williams, Explosive basaltic volcanism from Cerro Negro volcano: Influence of volatiles on eruptive style, *Science*, *277*, 1639–1642, 1997.
- Sakuyama, M., Petrology of arc volcanic-rocks and their origin by mantle diapirs, *J. Volcanol. Geotherm. Res.*, *18*, 297–320, 1983.
- Silver, L. A., Water in silicate glasses, Ph.D. thesis, Calif. Inst. of Technol., Pasadena, 1988.
- Sisson, T., and S. Bronto, Evidence for pressure-release melting beneath magmatic arcs from basalt at Galunggung, Indonesia, *Nature*, *391*, 883–886, 1998.
- Sisson, T. W., and T. L. Grove, Temperatures and H₂O contents of low-MgO high-alumina basalts, *Contrib. Mineral. Petrol.*, *113*, 167–184, 1993.
- Sisson, T. W., and G. D. Layne, H₂O in basalt and basaltic andesite glass inclusions from four subduction-related volcanoes, *Earth Planet. Sci. Lett.*, *117*, 619–635, 1993.
- Sobolev, A. V., Melt inclusions in minerals as a source of principle petrological information, *Petrology*, *4*, 209–220, 1996.
- Sobolev, A. V., and M. Chaussidon, H₂O concentrations in primary melts from supra-subduction zones and mid-ocean ridges: Implications for H₂O storage and recycling in the mantle, *Earth Planet. Sci. Lett.*, *137*, 45–55, 1996.
- Sobolev, A. V., and L. V. Danyushevsky, Petrology and geochemistry of boninites from the north termination of the Tonga trench: Constraints on the generation conditions of primary high-Ca boninite magmas, *J. Petrol.*, *35*, 1183–1211, 1994.
- Stern, R. J., On the origin of andesite in the northern Mariana Island Arc: Implications from Agrigan, *Contrib. Mineral. Petrol.*, *68*, 207–219, 1979.
- Stern, R. J., and L. D. Bibee, Esmeralda Bank: Geochemistry of an active submarine volcano in the Mariana Island Arc, *Contrib. Mineral. Petrol.*, *86*, 159–169, 1984.
- Stern, R. J., C. J. Jackson, P. Fryer, and E. Ito, Sr, Nd and Pb isotopic composition of the Kasuga cross-chain in the Mariana arc: A new perspective on the K-H relationship, *Earth Planet. Sci. Lett.*, *119*, 459–475, 1993.



- Stolper, E., Water in silicate glasses: An infrared spectroscopic study, *Contrib. Mineral. Petrol.*, *81*, 1–17, 1982.
- Stolper, E., and J. R. Holloway, Experimental determination of the solubility of carbon dioxide in molten basalt at low pressure, *Earth Planet. Sci. Lett.*, *87*, 397–408, 1988.
- Stolper, E., and S. Newman, The role of water in the petrogenesis of Mariana trough magmas, *Earth Planet. Sci. Lett.*, *121*, 293–325, 1994.
- Tingle, T. N., H. W. Green, and A. A. Finnerty, Experiments and observations bearing on the solubility and diffusivity of carbon in olivine, *J. Geophys. Res.*, *93*, 15,289–15,304, 1988.
- Vallier, T. L., G. A. Jenner, F. A. Frey, J. B. Gill, A. S. Davis, A. M. Volpe, J. W. Hawkins, J. D. Morris, P. A. Cawood, J. L. Morton, D. W. Scholl, M. Rautenschlein, W. M. White, R. W. Williams, A. J. Stevenson, and L. D. White, Subalkaline andesite from Valu Fa ridge, a back arc spreading center in southern Lau Basin: Petrogenesis, comparative chemistry, and tectonic implications, *Chem. Geol.*, *91*, 227–256, 1992.
- Watson, E. B., Diffusion of dissolved CO₂ and Cl in hydrous silicic to intermediate magmas, *Geochim. Cosmochim. Acta*, *55*, 1897–1902, 1991.
- Wopenka, B., J. D. Pasteris, and J. J. Freeman, Analysis of individual fluid inclusions by Fourier-transform infrared and Raman microspectroscopy, *Geochim. Cosmochim. Acta*, *54*, 519–533, 1990.
- Yamashita, S., T. Kitamura, and M. Kusakabe, Infrared spectroscopy of hydrous glasses of arc magma compositions, *Geochem. J.*, *31*, 169–174, 1997.
- Zhang, Y., E. M. Stolper, and G. J. Wasserburg, Diffusion of water in rhyolitic glasses, *Geochim. Cosmochim. Acta*, *55*, 441–456, 1991.